PIEZOELECTRIC MICROACTUATOR FAILURE DETECTOR SYSTEM FOR HARD DISK DRIVE

WITTHAYA KEOPUANG

A THESIS SUBMITTED IN PARTIAL FULFILLMENT
OF THE REQUIREMENT FOR THE DEGREE OF
MASTER OF ENGINEERING IN DATA STORAGE TECHNOLOGY
INTERNATIONAL COLLEGE
KING MONGKUT'S INSTITUTE OF TECHNOLOGY LADKRABANG
2013

KMITL-2013-IC-M-005-006

Thesis: Piezoelectric Microactuator Failure Detector System for Hard Disk Drive
Student: Mr. Witthaya Keopuang
Student ID: 52600630
Degree: Master of Engineering (M.E.)
Program: Data Storage Technology
Year: 2013
Thesis Advisor: Asst.Prof.Dr.Kasin Vichienchom
Co-Advisor: Asst.Prof.Dr.Kitiphol Chitsakul

ABSTRACT

Method and apparatus for detecting failure in a piezoelectric element on a head suspension for a disk drive is described. By clamping one end of the suspension, mechanically displacing and releasing the other end of the suspension produces electrical signal at the output of a piezoelectric element on the suspension. After being processed, characteristics of the signal are used to determine defects of its corresponding piezoelectric element and its circuit connectivity. The equipment based on the proposed method, the ePZT, was designed and tested against the Dynamic Electrical Tester (DET). The testing results show that the ePZT provides the same capability as the DET to detect and identify head failure due to its piezoelectric element fracture and broken electrical connection. Moreover, the ePZT possesses several advantages over DET such as low cost, faster operating time, and less space required. Therefore, it is suitable for using in production line.

Acknowledgement

This work is supported by Western Digital Thailand. The authors would like to thank Mr. Raymond Tan, HOD of HSA Product/Test engineer for his support and Dr. Yanning Liu, HOD of Mechanical engineering for his valuable suggestion on the topic, and Sanya Thamprasit, Siwaphon Sonkham for experiment supporting.

Contents

Contents (Cont.)

List of Table

List of Figures

List of Figures (Cont.)

Figure Page

List of Figures (Cont.)

Chapter 1
Introduction

1.1 Statement of Problem

Hard disk drive (HDD) is the most popular non-volatile, random-access mass data storage. Over the past several years, hard disk drive has been fallen in cost and physical size while dramatically increased in capacity. The biggest lever for higher HDD capacities is to increase both areal density and the number of disk per drive. A single disk can now store about 500 GB of data.

Increasing the areal density by reducing data track widths makes it more difficult to locate the read/write head accurately on the data tracks of the disk and keep maintaining. In order to overcome the problem, previous approach was introduction of voice coil motor (VCM), as well as the use of magnetic disks and head suspension with higher stiffness or rigidity. It is well recognized throughout the industry that these levels of performance cannot be simply achieved by an evolution of the existing voice coil positioning technologies. A feasible solution is to use a dual stage actuator (DSA). As the first stage control, VCM is still used for track locating. For micro positioning control, the second stage actuator based on piezoelectric (PZT) structure is employed. This second stage actuator is driven by the signals from the control electronics according to the off track error. Schematic of a hard disk drive with dual-stage actuator is illustrated in Fig. 1.1. The second stage actuator is mounted on suspension adjacent to read/write head. Its control signals are connected via flexure tails on a flexible printed circuit.

Higher number of disks per drive is another method to increase drive capacity. Since data is stored on both sides of the disk therefore it requires two read/write heads per disk. Typically, up to four disks are used thus it can be as much as eight heads and eight microactuators stack up as shown in Fig. 1.2. To minimize its occupying area, all actuators share the same control signal on the flexible printed circuit. As a result, all dual stage actuator circuits are connected in parallel. Since a piezoelectric can be modeled as a capacitor, the equivalent circuit of microactuators of a head stack assembly (HSA) is a parallel circuit of capacitors as shown in Fig. 1.3.

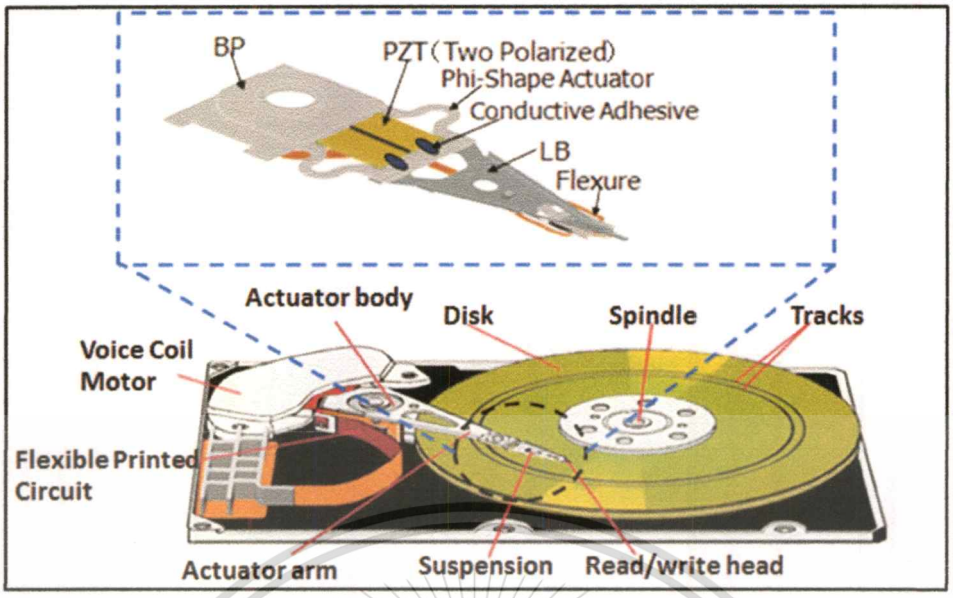

Fig. 1.1 Schematic of hard disk drive with dual stage actuator

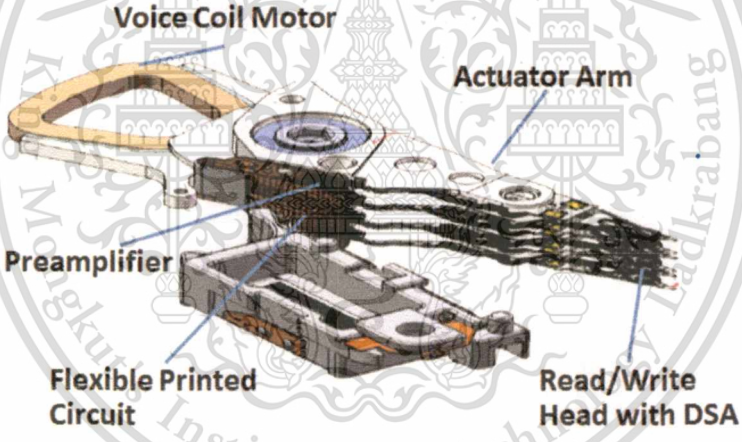

Fig. 1.2 View of head stack assembly

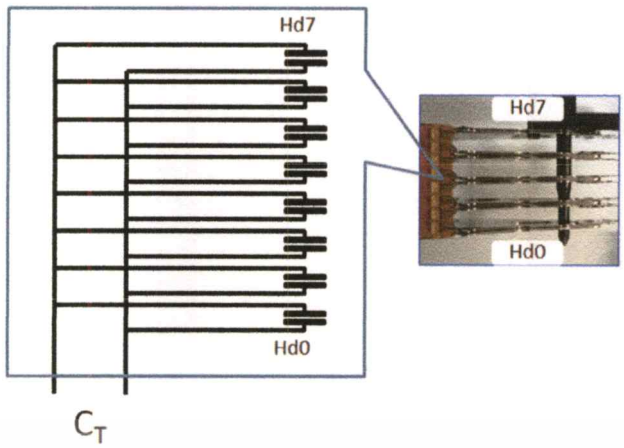

Fig. 1.3 Microactuators of a HSA connected in parallel are modeled as a parallel circuit of capacitors

Physical condition of the piezoelectric structure is directly related to the actuator performance and so the head performance. Conventionally, it can be primarily checked by measuring the value of its capacitance whether it is within its specification. However because of its nature of parallel circuit, only the total capacitance can be measured, thus it is insufficient to identify which dual stage actuator is prone to degrade head performance and eventually resulting in head failure.

In this research the method and apparatus for detecting failure in a piezoelectric element and its circuit connectivity of the HSA are described. The equipment was designed, tested and has been using for production line.

1.2 Objective of Study

To develop a method and a system that can be used to detect a non-functional microactuator in HSA due to PZT-actuated suspension failure.

To have a prototype tester for using in production line employing DSA (PZT attached at suspension). The tester must be low cost, simple to operate and provide the test result as accurate as the commercial tester.

1.3 Scope of Thesis

To design and develop a prototype tester which can identify the failed head of a Head Stack assembly (HSA) due to DSA connection open circuit and due to defection of PZT crack.

Chapter 2
Theory and Literature Review

2.1 Introduction

Piezoelectric materials have been developed and widely used in many fields of application. It is very important to understand its electro-mechanical effect. Therefore, the first part of this chapter will provide an overview of the piezoelectric phenomenon. Then a mathematical relationship of its electro-mechanical effect is formulated in the following section. The second part will explain about microactuator principle based on the application of piezoelectric element. Finally, a review and classification of the piezoelectric testing techniques will be covered in the last section.

2.2 The piezoelectric effect [1]

The word Piezoelectricity comes from Greek and means "electricity by pressure" (Piezo means pressure in Greek). This name was proposed by Hankel in 1881 to name the phenomenon discovered a year before by the Pierre and Jacques Curie brother. They observed that positive and negative charges appeared on several parts of the crystal surfaces when comprising the crystal in different directions.

Figure 2.1 shows a simple molecular model; it explains the generating of an electric charge as the result of a force exerted on the material. Before subjecting the material to some external stress, the gravity centers of the negative and positive charge of each molecule coincide. Therefore, the external effects of the negative and positive charges are reciprocally cancelled. As a result, an electrically neutral molecule appears. When exerting some pressure on the material, its internal reticular structure can be deformed, causing the separation of the positive and negative gravity centers of the molecule and generating little dipoles as illustrated in Fig. 2.2. The facing poles inside the material are mutually cancelled and a distribution of a linked charge appears in the material's surface as illustrated in Fig. 2.3. That is to say, the material is polarized. This polarization generates and electric field and can be

used to transform the mechanical energy used in the material's deformation into electrical energy.

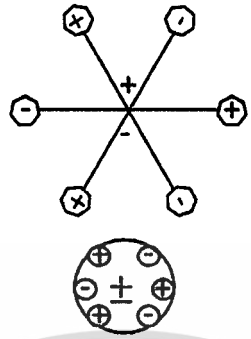

Fig. 2.1 Unperturbed molecule

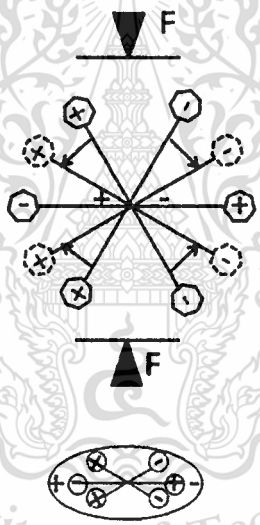

Fig. 2.2 Molecule subjected to an external force

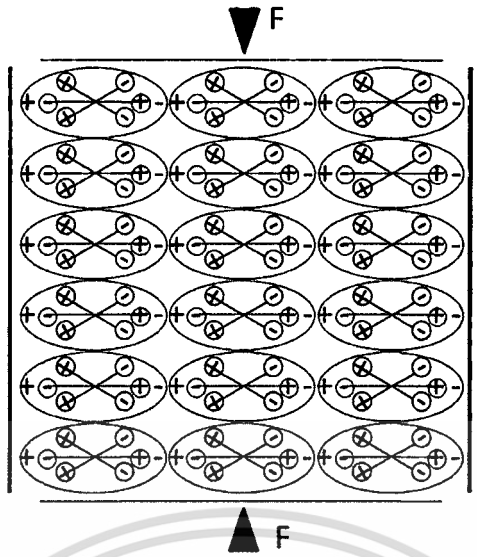

Fig. 2.3 Polarizing effect on the material surfaced

Figure 2.4 shows the piezoelectric material on which a pressure is applied. Two metal plates used as electrodes are deposited on the surfaces where the linked charges of opposite sign appear. Suppose that those electrodes are externally short-circuited through a wire to which a galvanometer has been connected. When exerting some pressure on the piezoelectric material, a linked charge density appears on the surfaces of the crystal in contact with the electrodes. This polarization generates an electric field which causes the flow of the free charges existing in the conductor. Depending on their sign, the free charges will move towards the ends where the linked charge generated by the crystal's polarization is of opposite sign. This flow of free charges will remain until the free charge neutralizes the polarization effect. When the pressure on the crystal stops, the polarization will disappear, and the flow of free charges will be reversed, coming back to the initial standstill condition. It shows in Fig. 2.5. This process would be displayed in the galvanometer, which would have marked two opposite sign current peaks. If a resistance is connected instead of a short-circuiting, and a variable pressure is applied, a current would flow through the resistance, and the mechanical energy would be transformed into electrical energy.

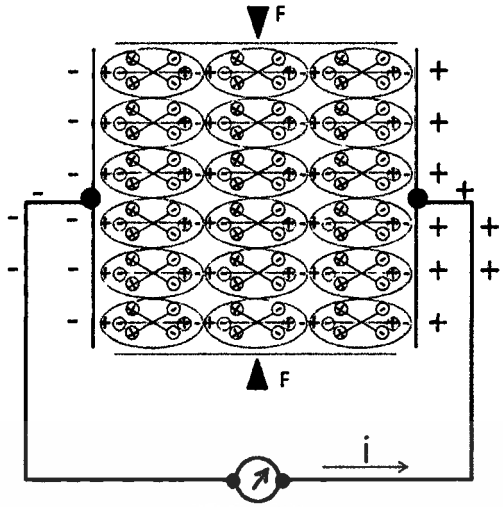

Fig. 2.4 Neutralizing current flowing through the short-circuiting established on a piezoelectric material subjected to an external force

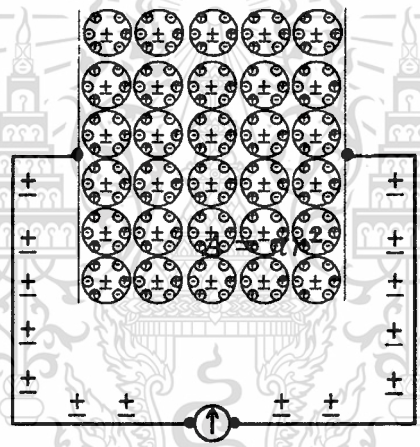

Fig. 2.5 Absence of current through the short-circuited material in an unperturrbed state

The Curie brothers verified, the year after their discovery, the existence of the reverse process, predicted by Gabriel Lippmann (1881). That is, if one arbitrarily names direct piezoelectric effect, to the generation of an electric charge, and hence of an electric field, in certain materials and under certain laws due to a stress, there would also exist a reverse piezoelectric effect by which the application of an electric field, under similar circumstances, would cause deformation in those materials

In this sense, a mechanical deformation would be produced in a piezoelectric material when a voltage is applied between the electrodes of the piezoelectric material, as shown in Fig. 2.4 and Fig. 2.5. This strain could be used, for example, to

displace a coupled mechanical load, transforming the electrical energy into mechanical energy.

2.2.1 Mathematical formulation of the piezoelectric effect

In a first approach, the experiments performed by the Curie brothers demonstrated that the surface density of the generated linked charge was proportional to the pressure exerted, and would disappear with it. This relationship can be formulated in a simple way as follows:

$$P_p = dT \tag{1.1}$$

Where P_p is the piezoelectric polarization vector, whose magnitude is equal to the linked charge surface density by piezoelectric effect in the considered surface, **d** is the piezoelectric strain coefficient and T is the stress to which the piezoelectric material is subjected. The Curie brothers verified the reverse piezoelectric effect and demonstrated that the ratio between the strain produced and the magnitude of the applied electric field in the reverse effect, was equal to the ratio between the produced polarization and the magnitude of the applied stress in the direct effect. Consistently, the reverse piezoelectric effect can be formulated in a simple way, as a first approach, as follows:

$$S_p = dE \tag{1.2}$$

Where S_p is the strain produced by the piezoelectric effect and E is the magnitude of the applied electric field. The direct and reverse piezoelectric effects can be alternatively formulated, considering the elastic properties of the material, as follows:

$$P_p = dT = dcS = eS \tag{1.3}$$

$$T_p = cS_p = cdE = eE \tag{1.4}$$

Where c is the elastic constant, which relates the stress generated by the application of a strain (T = c S), s is the compliance coefficient which relates the deformation produced by the application of a stress (S = s T), and e is the piezoelectric stress constant. (Note that the polarizations, stresses, and strains caused by the piezoelectric effect have been specified with the p subscript, while those externally applied do not have subscript. Although unnecessary, it will be advantageous later on.

2.2.2 Piezoelectric contribution to elastic constants

The piezoelectric phenomenon causes an increase of the material's stiffness. To understand this effect, let us suppose that the piezoelectric material is subjected to a strain S. This strain will have two effects. On the one hand, it will generate an elastic stress T_e which will be proportional to the mechanical strain $T_e = c\,S$; on the other hand, it will generate a piezoelectric polarization $P_p = e\,S$ according to Eq. (1.3). This polarization will create an internal electric field in the material E_p given by

$$E_p = \frac{P_p}{\varepsilon} = \frac{eS}{\varepsilon} \tag{1.5}$$

Where ε is the dielectric constant of the material. This electric field, of piezoelectric origin, produces a force against the deformation of the material's electric structure, creating a stress $T_p = e\,E_p$. This stress, as well as that of elastic origin, is against the material's deformation. Consistently, the stress generated as a consequence of the strain S will be:

$$T = T_e + T_p = cS + \frac{e^2}{\varepsilon}S = \left(c + \frac{e^2}{\varepsilon}\right)S = \bar{c}S \tag{1.6}$$

Therefore, the constant $\bar{c}$ is the piezoelectrically stiffened constant, which includes the increase in the value of the elastic constant due to the piezoelectric effect. This coefficient will appear later on.

2.2.3 Piezoelectric contribution to dielectric constants

When an external electric field E is applied between two electrodes where a material of dielectric constant ε exists, an electric displacement is created towards those electrodes, generating a surface charge density $\sigma = \sigma_o + \sigma_p$ which magnitude is $D = \varepsilon E$. If that material is piezoelectric, the electric field E produces a strain given by: $S_p = d\,E$. This strain of piezoelectric origin increases the surface charge density due to the material's polarization in an amount given by: $P_p = e\,S_p = e\,d\,E$ (Fig. 2.6) Because the electric field is maintained constant, the piezoelectric polarization increases the electric displacement of free charges towards the electrodes in the same magnitude ($\sigma_p = P_p$). Therefore, the total electrical displacement is:

$$D = \varepsilon E + P_p = \varepsilon E + edE = \bar{\varepsilon} E \qquad (1.7)$$

where $\bar{\varepsilon}$ is the effective dielectric constant which includes the piezoelectric contribution.

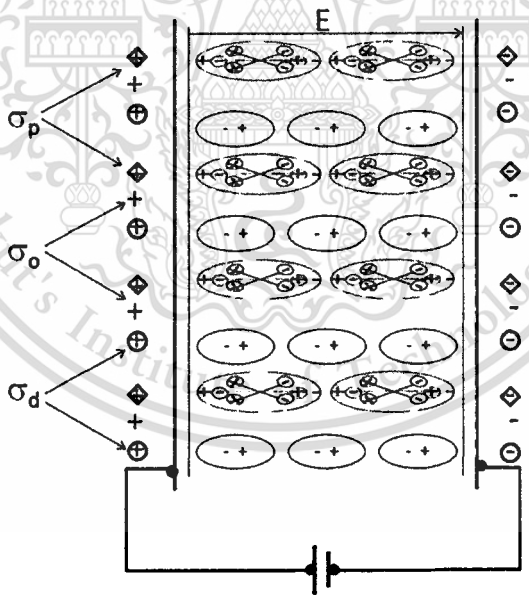

Fig. 2.6 Schematic diagram that explains different electrical displacements associated with a piezoelectric and dielectric material

2.2.4 The electric displacement and internal stress

As shown in the previous paragraph. The electric displacement produced when an electric field **E** is applied to a piezoelectric and dielectric material is:

$$D = \varepsilon E + P_p = \varepsilon E + eS_p \tag{1.8}$$

Under the same circumstances, we want to obtain the internal stress in the material. The reasoning is the following: the application of an electric field on a piezoelectric material causes a deformation in the material's structure given by: $S_p = d\,E$. This strain produces an elastic stress whose magnitude is $T_e = c\,S_p$. On the other hand, the electric field **E** exerts a force on the material's internal structure generating a stress given by: $T_p = e\,E$. This stress is, definitely, the one that produces the strain and is of opposite sign to the elastic stress which tends to recover the original structure. Therefore, the internal stress that the material experiences will be the resultant of both. That is:

$$T = cS_p - eE \tag{1.9}$$

Eventually, both stresses will be equal leaving the material strained and static. If a variable field is applied, as it is the common practice, the strain will vary as well, producing a dynamic displacement of the material's particles. This electromechanical phenomenon generates a perturbation in the medium in contact with the piezoelectric material. This effect is used in transducers, sensors and actuators.

2.2.5 Basic model of electric impedance for a piezoelectric material subjected to a variable electric field

In the previous section, the expressions for the electric displacement and the internal stress produced in a piezoelectric material subjected to an electric field have been obtained. The electric field is created when a voltage difference is applied between two electrodes deposited on certain surfaces of the material. If the applied voltage difference changes, the electric field as well as the electric displacement change inducing an electric current through the electrodes.

The ratio between the applied voltage and the induced electric current is the electrical impedance of the piezoelectric component. For example, if it only has

dielectric properties, the resulting electrical impedance corresponds to a capacitance. Piezoelectric devices are included in electric and electronic circuits to use their electromechanical properties in both direct and reverse applications. Therefore, it is important to obtain an electric model that allows including the piezoelectric component in electric circuits. This will greatly facilitate the analysis of the circuit and the understanding of its operation.

Next, the basic equivalent electric model mentioned will be obtained. In the obtaining of the model some simplifications will be made to minimize the mathematical formulation. These simplifications do not essentially modify the results and let us show the qualitative physical concepts of the model. On the other hand, the obtained expressions for the electric parameters of the model will be very similar to those obtained from a more rigorous mathematical development.

Figure 2.7 shows the transversal section of a bar of piezoelectric material of thickness l. Let us suppose that when applying a field in the direction of the thickness (direction Y) by the application of a voltage difference between the electrodes, the material deforms as shown in the left part of Fig. 2.7. When the field is reversed, the strain is reversed as well (right part).

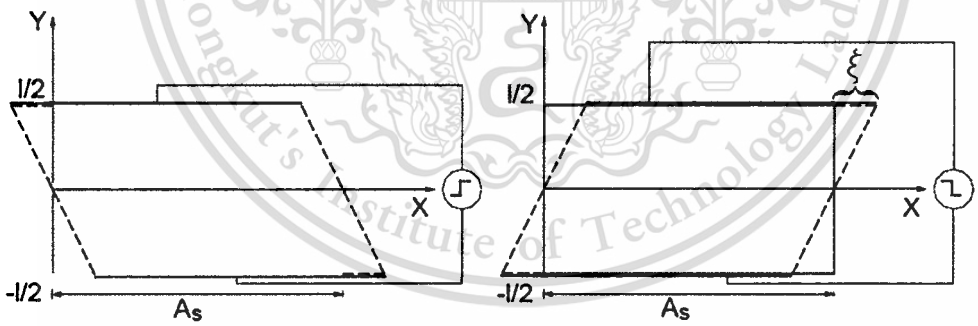

Fig. 2.7 Shear strains produced in a piezoelectric material subjected to a reverting voltage

The strain is produced when displacement gradients occur, or in other words, when the particles displacement increases or decreases in one direction. Therefore, the strain S is defined as the gradient of the particles displacement in the direction considered. Thus, if the displacement that the particles experience along a distance y is $\xi(y)$, the strain produced along this section will be:

$$S(y) = \frac{\xi(y)}{y} \tag{1.10}$$

Figure 2.7 shows how the particles displacement increases with the coordinate y, being null on the abscissas axis. Consistently, the maximum strain is produced at y = l/2 and is the same in both ends but of opposite sign due to the change of sign in the displacement. Therefore, the strain at y=l/2 will be:

$$S\,(l/2) = \frac{\xi}{l/2} = \frac{2\xi}{l} \tag{1.11}$$

Where ξ is the particle displacement at the coordinate y=l/2 at a generic instant.

Figure 2.8 shows the forces acting on the material ends when the electric field is applied. This electric field creates a force in the X direction which produces a piezoelectric stress given by Eq. (1.4). An elastic stress $T_e = cS_p$ is against the piezoelectric stress and tries to avoid the strain of the material. The internal friction that the particles experience in their displacement is also against the piezoelectric stress since it makes the particles displacement more difficult. The stress due to internal friction is usually considered proportional to the gradient of the particle displacement velocity, as in the case of a viscous phenomenon, that is:

$$T_v = \eta \frac{dv}{dy} = \eta \frac{d^2\xi}{dy\,dt} = \eta \frac{dS}{dt} \tag{1.12}$$

where constant η is named viscosity.

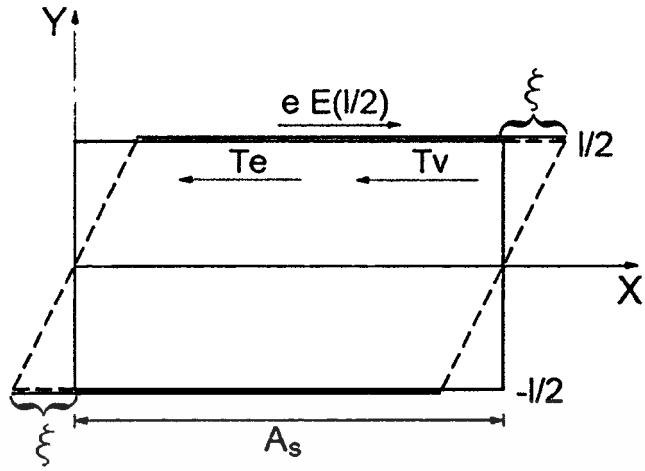

Fig. 2.8 Shear strain and stresses produced at the end of a piezoelectric plate subjected to an electric field

The resultant of the forces will be equal to the product of mass by the acceleration of the particles. As stresses are being considered, it will be necessary to take into account the surface mass density ρ_s. Therefore, Newton's first law applied to the material surface at the coordinate y=1/2 will be:

$$\sum T = eE(l/2) - cS(l/2) - \eta \frac{dS(l/2)}{dt} = \rho_s \frac{d^2\xi}{dt^2} \qquad (1.13)$$

Considering Eq. (1.11), Eq. (1.13) and that E(l/2) = V/l, where V is the voltage difference between the electrodes, the following expression for the voltage V is obtained:

$$V = \frac{2\eta}{e}\frac{d\xi}{dt} + \frac{\rho_s l}{e}\frac{d^2\xi}{dt^2} + \frac{2c}{e}\xi \qquad (1.14)$$

On the other hand, the electric displacement on the electrodes is given by Eq. (1.8). The time derivative of the electric displacement provides the density of the induced current J given by:

$$J = \frac{dD(l/2)}{dt} = \varepsilon\frac{dE(l/2)}{dt} + e\frac{dS(l/2)}{dt} = J_d + J_p \qquad (1.15)$$

The first term J_d corresponds to the density of the induced current by the dielectric effect and the second term J_p to the current induced by the piezoelectric effect. Let us analyze the second term, which can be written from Eq. (1.11) as:

$$J_p = \frac{2e}{l}\frac{d\xi}{dt} \tag{1.16}$$

Taking into account that the surface density current $J_p = i_p/A_S$, where i_p is the current induced by piezoelectric effect and A_S is the electrodes surface, the following relationship can be obtained from Eq. (1.16):

$$\frac{d\xi}{dt} = \frac{l}{2eA_S} i_p \tag{1.17}$$

By substituting Eq. (1.17) in Eq. (1.14), it is definitely obtained:

$$V = \frac{\eta l}{A_S e^2} i_p + \frac{\rho_S l^2}{2A_S e^2}\frac{di_p}{dt} + \frac{cl}{A_S e^2}\int i_p dt \tag{1.18}$$

The voltage arising between the ends of a series circuit formed by a resistance R_m, an inductance L_m and a capacitance C_m through which an i_p current flows, has the following expression:

$$V = R_m i_p + L_m \frac{di_p}{dt} + \frac{1}{C_m}\int i_p \, dt \tag{1.19}$$

Therefore, the current induced by the piezoelectric effect, i.e., by the electromechanical effect, in the material is the same as the one that would flow through a series electric circuit formed by a resistor, a coil and a capacitor with the following magnitudes of resistance, inductance and capacitance, respectively:

$$R_m = \frac{\eta l}{Ae^2} = K_R \eta,$$
$$L_m = \frac{\rho_S l^2}{2Ae^2} = K_L \rho_S,$$

$$C_m = \frac{Ae^2}{cl} = K_C \frac{1}{c} = K_C s$$

The former expressions make clear the relationships among the electrical parameters and mechanical properties of the material, which are: the resistive electric parameter is proportional to the viscosity and models the physical phenomenon of energy loss due to viscous effects. The inductive parameter is proportional to the surface mass density and models the energy storage by inertial effect, and the capacitive parameter which is proportional to the elastic compliance models the energy storage by elastic effect. These relationships, which settle a clear analogy between the physical properties and the electric parameters, are very useful when evaluating the physical phenomena which take place when the piezoelectric material is used as a micro-gravimetric sensor.

Apart from the i_p component, it is also necessary to consider the component i_d associated with the dielectric effect. In fact, it can be written from Eq. (1.15) as follows:

$$i_d = A_S J_d = A_S \varepsilon \frac{dE(l/2)}{dt} = \varepsilon \frac{A_S}{l} \frac{dV}{dt} \qquad (1.20)$$

Eq. (1.20) corresponds to the current induced through a capacitor $C_o = \varepsilon A_S / l$ when a variable voltage difference V is applied. Consistently, the circuit that models the electrical impedance of a piezoelectric and dielectric material subjected to a variable voltage difference is shown in Fig. 2.9. The electric circuit is formed by two parallel branches: one of them is the so-called motional branch formed by a series R_m L_m C_m circuit that models the motional physical phenomenon. The other is the so-called static branch formed by a capacitor C_o which is associated to the electrical capacitance arising from the dielectric material placed between the two electrodes.

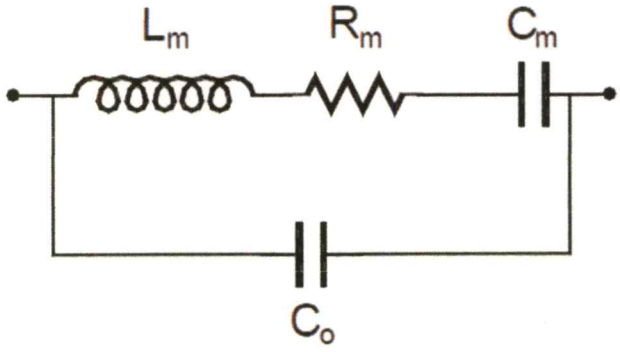

Fig. 2.9 Equivalent electrical model of a piezoelectric material vibrating at frequencies near resonance

2.3 Microactuator principle

As higher recording density and transfer rate of HDDs are required, track densities and spindle rotation speed are being rapidly increased. As the track width is becoming narrower, it has become extremely difficult for the head to precisely trace a specific track owing to turbulence and disk vibration even at higher frequencies. In order to overcome the problem, previous approach was introduction of fluid dynamics spindle motors, as well as the usage of magnetic disks and head suspension with higher stiffness or rigidity.

Another noticeable technology for the problem solution is DSA. Roughly divided, there have been three types of DSAs proposed and developed so far. The first one is the type which drives and swings the suspension to precisely position the head element. The second type is the one in which a microactuator placed between the gimbals and head slider positions the head element without driving the suspension. The second type is advantageous in acquiring higher frequency response since the mass of the driving portion can be designed small. The third type is the one, which drives the head element itself without driving the slider or the suspension. Among those three, the first type is ready to be industrialized. The second type is the one, which is most widely and intensively researched.

Figure 2.10 shows the perspective illustration of the head gimbal assembly. Conventional ones for the current HDDs use are available. The head motion is controlled by a PZT microactuator elements as shown in Fig. 2.11. By applying to the two PZT elements alternating voltage with opposite phase to each other, the head slider rotates around the dimple pivot on the suspension.

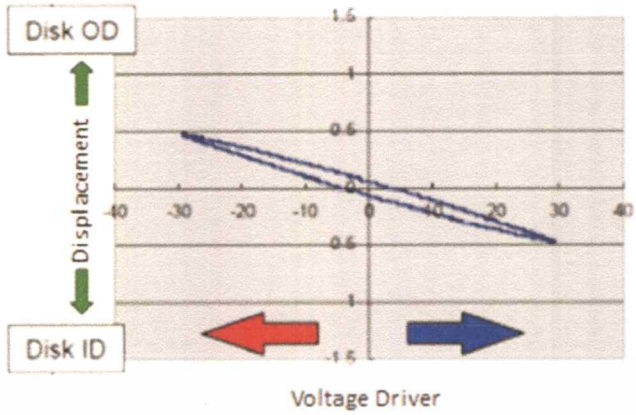

Fig. 2.10 Head gimbal assembly

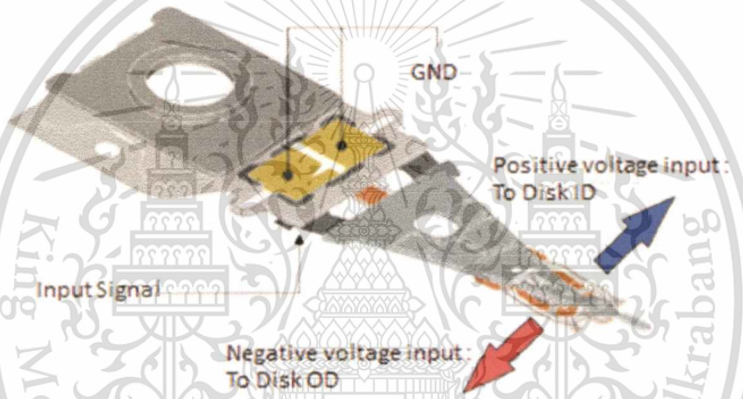

Fig. 2.11 The head motion is controlled by a pair of PZT microactuator elements

Known testing approaches for identifying microactuator failures include resistance test and stroke test. There remains, however, a continuing need for improve microactuator failure test methods and associated systems. Methods and system which are capable of being efficiently performed and which can accurately identify a wide range of failures would be particularly desirable.

2.4 Existing methods for testing microactuator

Disk drive component manufacturers typically test the various components of the disk drive before they are incorporated into assemblies or sub-assemblies. The piezoelectric actuators are among the many aspects of a head-arm assembly or HSA that must be tested. Several methods exist for testing microactuators that include piezoelectric materials. These methods generally include, measuring capacitance,

performing visual checks, measurement of a mechanical displacement or stroke by a Laser Doppler Vibrometer (LDV) or Dynamic Electrical Tester (DET), electrical test and applying mechanical force into piezoelectric element while monitoring its electrical signal.

2.4.1 Capacitance test

This method is based on the assumption that there are capacitors in the equivalent electrical model of piezoelectric material. If there is any physical damage on the piezoelectric thin film, its equivalent capacitance will be altered. Practically, if there is a crack on the piezoelectric thin film, its capacitance will fall down. Therefore measuring the capacitance of the piezoelectric microactuator through its control circuit and comparing it to the nominal value can provide this information. This technique was used in [2] where the dual stage actuator with piezoelectric thin film was designed and evaluated whether there were any cracks developed after the mechanical shock test. Another example of using capacitance test is in [3]. In this case before performing capacitance measurement using AC source, it needs to stabilize the resistance value of the conductive resin such as silver paste on the piezoelectric body by biasing with a DC voltage until dielectric breakdown occurs in the conductive resin.

In addition, capacitance measurement can provide the information about conditions of the connectivity of the microactuator control circuit such as short circuit and open circuit. Although the capacitance testing is straightforward and quite reliable, it is not suitable for HSAs which consist of multiple head. This because HSAs with multiple heads share the same microactuator control circuit, thus effectively, multiple piezoelectric microactuators are connected in parallel. The capacitance measured is indeed the sum of them. The sum of the capacitance value can be within reference value range while its individual value is unacceptable. As a result, it is possible that a HSA with a degraded piezoelectric microactuator may pass its inspection. On the other hand, if the sum of the capacitance measured is out of the reference value range, still this technique cannot identify which head whose piezoelectric microactuator is degraded.

2.4.2 Displacement test by Laser Doppler Vibrometer (LDV)

LDV has been extensively used as the standard instrument for measurement and analysis head positioning and displacement such as in [4]-[6]. There are several advantages of using LDV. It is a non-contact measurement thus reduces the risk of damaging the subject which is the read/write head in this case. Because of using laser, it can be directed to the read/write head that is difficult to access. In the displacement test, an HGA's microactuator is driven with a low frequency AC voltage, typically in a range of few kHz. The LDV's laser beam is directed at the head area. The reflected light is collected and analyzed for the displacement of the reflecting surface. The displaced amount and the response speed of the microactuator in response to the applied signal can be accurately measured. If the piezoelectric microactuator and its control circuit function correctly, the displacement will be within its specification. The LDV can measure the head displacement with a very high accuracy at a resolution level of sub micrometer. Measurement results typically show as Lissajous' plot of head displacement versus applied AC voltage as illustrated in Fig. 2.12

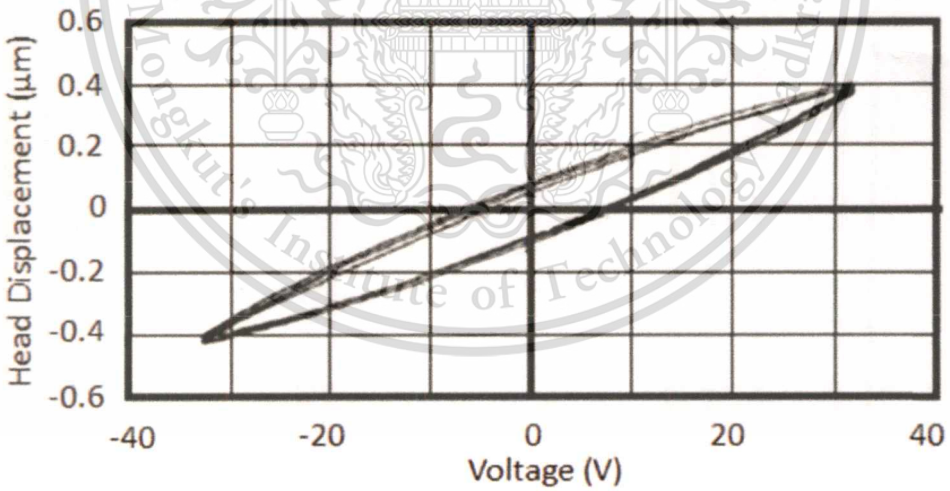

Fig. 2.12 Lissajous' plot of head displacement vs. applied voltage at 1 kHz [6]

Technically, displacement test using LDV can be applied for testing a HSA by scanning each head that shares the same control circuit sequentially. However, during manufacturing and testing processes of an HSA, such displacement measurement will cause the following various problems:

1). Because the LDV system is very expensive, a manufacturing cost of the HSA will increases tremendously;

2). A long measurement time of LDV system increases the inspection time of the testing process thus cost of testing which is a part of the manufacturing cost also to increase;

3). Introduction of LDV system which is not included in the normal inspection instruments for testing the magnetic head element will complicate the inspection process and also increase the number of step of the inspection process;

4). The LDV system increases the footprint of the inspection instruments of the production line. More space to install is required.

2.4.3 Displacement or stroke test by Dynamic Electrical Test (DET)

This method requires a very expensive system called dynamic electrical tester (DET) or dynamic parametric tester (DPT). The DET/DPT system consists of a stand for disk spinning and a mounting place for the tested HGA or HSA which is connected to electronic and control circuits. During the media spinning, the system writes and reads signals to and from the media, measures, analyzes and reports some parameters such as Amplitude, Pulse width, Overwrite, Signal to Noise ratio according to the test setup. The DET system can be used for testing the stroke and frequency response of a microactuator as described in [7]. The technique can be explained as follows. First, the DET writes two concentric tracks on a noise free portion of a magnetic storage medium at a pre-determined pitch. Track profile of the two concentric tracks is obtained by reading at successively increasing or decreasing radii. Each peak of the track profile indicates a center of a track. A magnetic read/write head and a microactuator is then positioned between the two concentric tracks. An AC signal at a desired frequency is applied to the microactuator while reading back a signal from the two concentric tracks. By comparison the read-back signal to the track profile, a stroke characteristic of the microactuator at this particular frequency can be determined. To obtain the frequency response of the microactuator, the same procedure can be repeated at other frequencies. The procedure of stroke characterization using DET is depicted in Fig. 2.13.

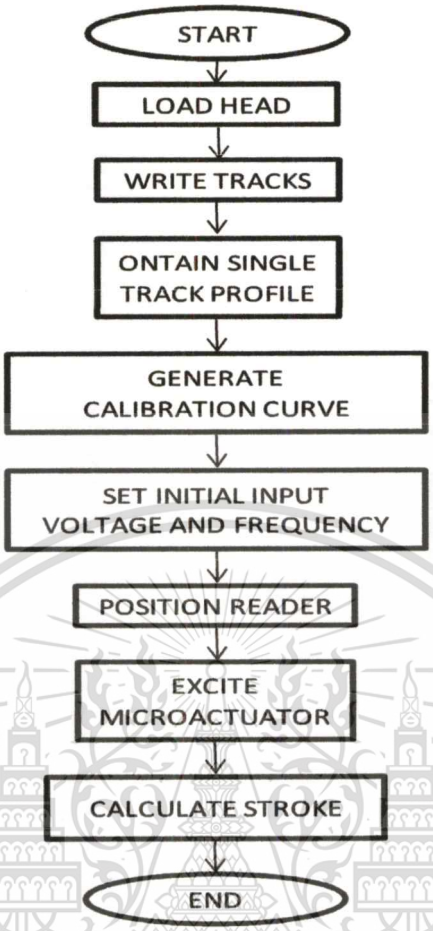

Fig. 2.13 The procedure of stroke characterization using DET [7]

In [8] another way of using DET to characterize microactuator was reported. In this technique, the head is positioned over a track on a disk based in part on servo information read from the disk. Input signal is applied to the microactuator on the suspension assembly. Servo information is then read from the disk to determine a change in the position of the head. By comparing the change in the position of the head to the input signal applied to the microactuator, a performance characteristic of a microactuator can be determined. The flowchart of testing procedure and the transfer characteristic between the input signal and the position of the head is shown in Fig. 2.14 and Fig. 2.15 respectively.

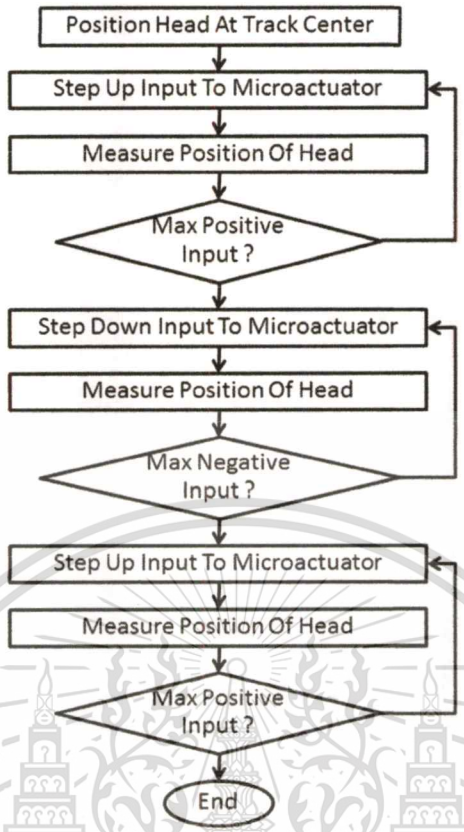

Fig. 2.14 Testing procedure of microactuator characterization [8]

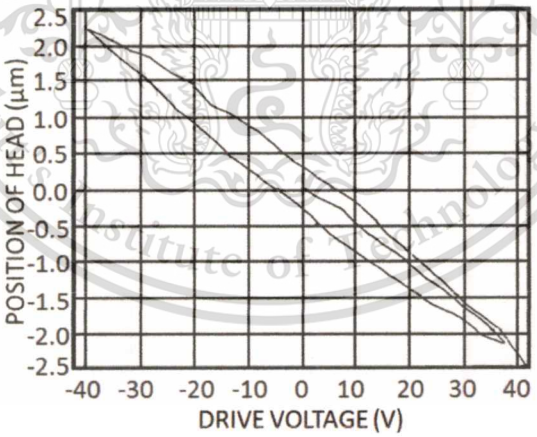

Fig. 2.15 Example of a transfer characteristic between input signal to the microactuator and position of the head as perform measurement [8]

Measurement using DET system not only gives a very accurate displacement but provides a frequency response of the microactuator as well. Furthermore, it can apply to both HGA and HSA. However the test result of this technique highly depends on the writing and reading performance of the head and its circuitry.

Because it does not exclusively measure the performance of the microactuator, it is possible that a HGA or HSA fails the displacement test due to the flaw in either writing or reading process instead of the defect from microactuator. Similar to LDV system, DET system is very expensive, requires a long test time, and occupies a large area. Consequently it is not suitable for using in production line.

2.4.4 Electrical test

There are several methods of detection that involve of exciting piezoelectric element by either electrical signal or mechanical force and then measuring its electrical response. They are classified as the electrical test and will be reviewed as follows.

Wei Guo et al [9] developed a test method for testing of a disk drive microactuator that includes two piezoelectric elements by providing a reference signal (electrical signal) to one of the piezoelectric element in the microactuator and obtaining a response signal from the other of the piezoelectric element. The response signal or the test measure of the device under test is then compared to its predetermined measure to determine if there is any defect. As shown in Fig. 2.16, the same response is produced in the case of a functional microactuator.

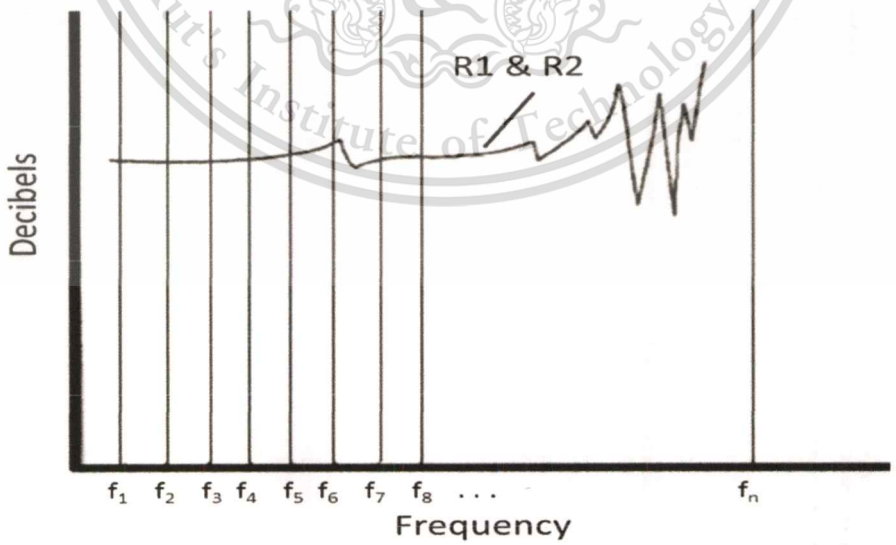

Fig. 2.16 Comparison of a test measure (R1) with a predetermined measure (R2) of an functional microactuator [9]

For a degraded or non-functional microactuator, a noticeable distinction between two responses can be found as in Fig. 2.17.

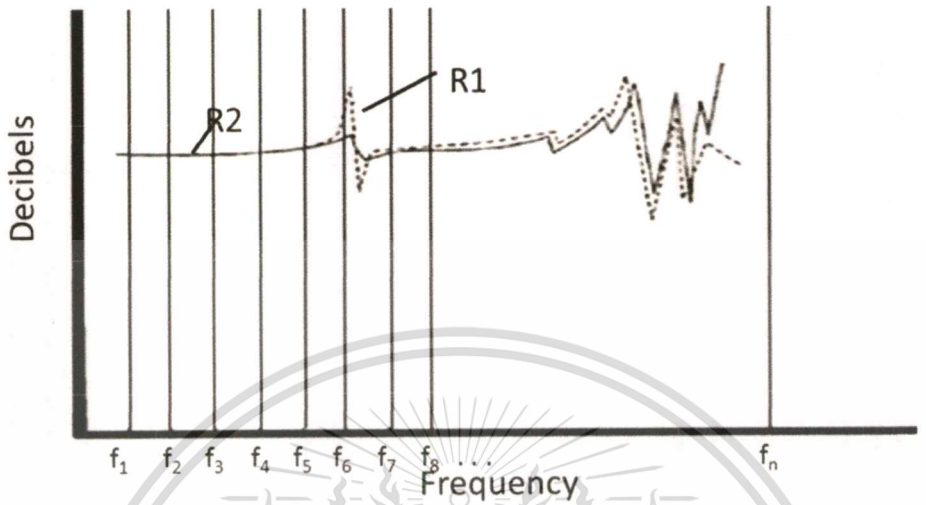

Fig. 2.17 Comparison of a test measure (R1) with a predetermined measure (R2) of an defected microactuator. There are substantial distinctions between R1 and R2 as the resonance characteristics of the piezoelectric element have changed [9]

Similarly, Umanskiy et al [10] developed a method for detecting defect in piezoelectric actuator by applying a single DC voltage pulse across the piezoelectric element. The duration of the pulse must be long enough for it to achieve a significantly steady state mechanical distortion. The sudden termination of the voltage across the piezoelectric element causes it to oscillate and decay freely. As the voltage continues to decay slowly, and the oscillations continues to decay in magnitude as well, providing a relatively complex signal from which features can be extracted and compared to those of known-good devices as shown in Fig. 2.18 and Fig. 2.19.

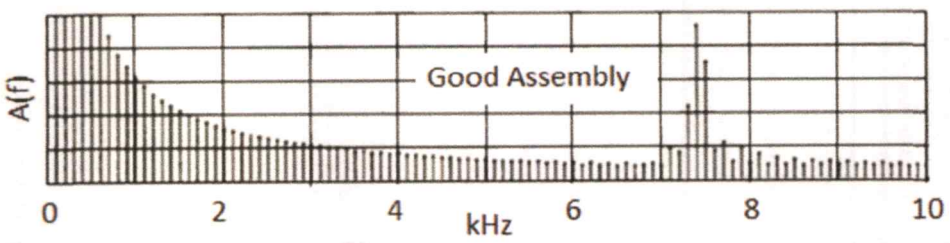

Fig. 2.18 Frequency domain profile corresponding of the known good assembly [10]

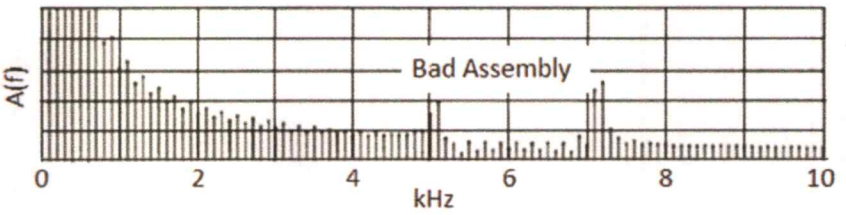

Fig. 2.19 Frequency spectrum corresponding of the known bad assembly [10]

Another method of testing and analysis employing pulse excitation was described in [11]. An electric pulse was applied to the piezoelectric transducer, by a square wave generator. The supplied electrical pulse must have a very short time of transit because the piezoelectric material emits a decay signal when the electrical pulse is applied and another decay signal when the electrical pulse is stopped. The piezoelectric transducer signal and the square wave impulse travel to the input of threshold rectifier. While the piezoelectric transducer signal is amplified, the square wave impulse is reduced to the threshold limit of a rectifier. This leaves the piezoelectric transducer signal as the only signal at the output of the amplifier, all aspects of the square wave pulse having been eliminated. This signal is directly proportional to the quality of the piezoelectric material as a transducer. The concept of this technique is shown in Fig. 2.20.

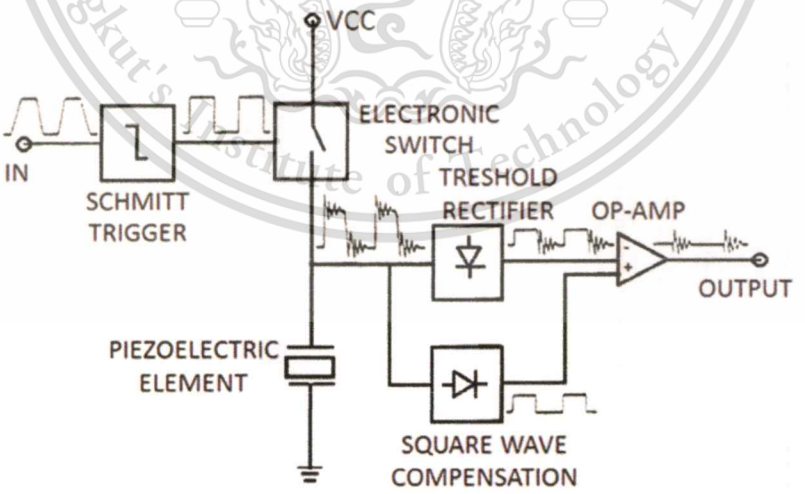

Fig. 2.20 Schematic for analysis of the transducer output signal [11]

In [12] a non-contact technique based on impedance measurement for testing piezoelectric actuators was proposed as shown in Fig. 2.21.

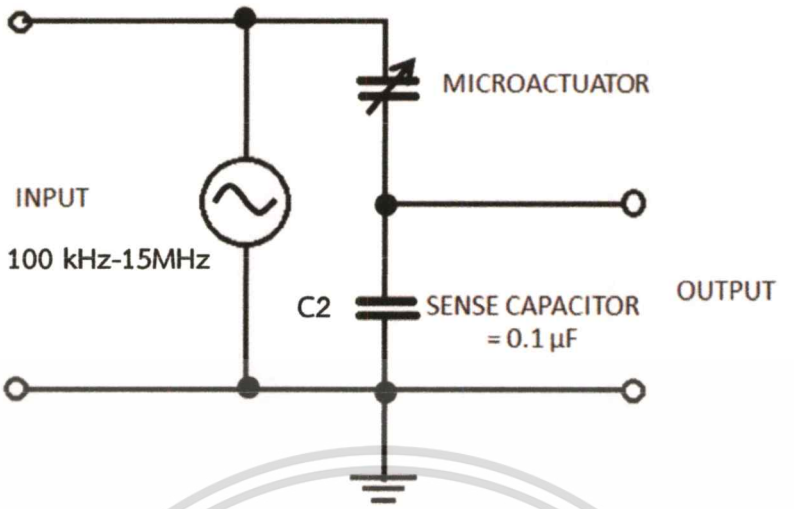

Fig. 2.21 Impedance test circuit [12]

Figure 2.21 shows the circuit design of the impedance test. C2 is a mono-block capacitor with a value of 0.1 micro-Farad and 50 Volts. An HP analyzer 4396A (100 kHz–1.8 GHz) was used to create a sweep sine frequency between 100 kHz to 15 MHz and measure a frequency response of piezoelectric transducer.

The electrical tests that have been reviewed so far are non-contact testings and demand short test time. Thus, they can be included in mass manufacturing. However, those methods have a major drawback. Because microactuator circuits of a HSA which is comprised of multiple heads are connected in parallel manner, they are unable to identify failure at each location of piezoelectric.

Finally, it is also possible to excite to the piezoelectric element mechanically and analyze its electrical response. Such a method is described in [13] and shown in Fig. 2.22. By clamping one end of the suspension and mechanically displacing and rapidly releasing the other end of the suspension, electrical output signal of a piezoelectric element on the suspension can be generated. Analysis and comparison of the output signal in frequency domain with a predetermined output can provide information about the microactuator condition. Likewise, this method is not applicable for multiple head manufacturing process. Moreover, there is a chance of damaging head if an excessive mechanical force is applied.

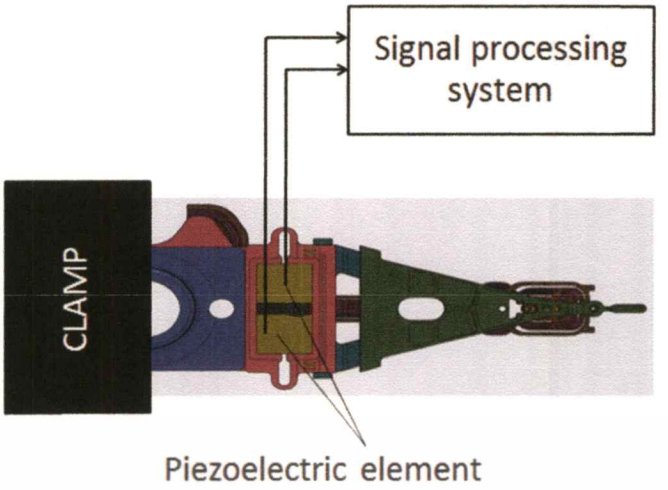

Fig. 2.22 Schematic of a microactuated suspension with a motor failure detection system [13]

2.5 Summary

Piezoelectric materials have been technically employed for long time. Their components are well established in many fields of applications due to its fast electromechanical response and compact size. Electromechanical response of piezoelectric can be used for sensing stresses and produce strains or displacements.

As higher recording density HDDs is required, a microactuator was introduced to achieve a precision head control. This microactuator is made of piezoelectric material since it generates displacement by its own contraction or expansion. It is mounted to the suspension. The piezoelectric material is brittle. During the assembly process, it is susceptible to some mechanical forces that can create defects such as a crack on it. Therefore, it is of importance to detect this degraded or failed microactuator.

In this chapter a number of testing approaches for identifying microactuator failures have been reviewed including capacitance test, displacement measurement by LDV and DET, and some electrical tests. All of them can use to detect the failure of piezoelectric but lack of location identifying, thus suitable for HGA testing only. Furthermore, some of them are time-consuming and require a large testing area. As a result, they are costly to implement in production line.

Chapter 3
Methodology and Experiment

3.1 Introduction

A huge market exists for hard disk drives for mass-market host computer systems such as servers, desktop computers, and laptop computers. To be competitive in this market, a hard disk drive must be relatively inexpensive, and must accordingly embody a design that is adapted for low-cost mass production. In addition, it must provide substantial capacity, rapid access to data, and reliable performance. Many manufacturers compete in this huge market and collectively conduct substantial research and development, at great annual cost, to design and develop innovative hard disk drives to meet increasingly demanding customer requirements.

The storage capacity of the hard disk drive can be increased by increasing the track density (TPI) on the disk and/or by including additional disks in a disk stack. Increasing the recording and reproducing density of the information tracks on the disks by using a narrower track width or a narrower track pitch. However, each increase in track density requires that the disk drive device have a corresponding increase in the positional control of the read/write head in order to enable quick and accurate reading and writing operations using the higher density disks. As track density increases, it becomes more and more difficult to quickly and accurately position the read/write head over the desired information tracks on the disk. Thus, disk drive manufacturers are constantly seeking ways to improve the positional control of the read/write head in order to take advantage of the continual increases in track density.

One approach that has been effectively used by disk drive manufacturers to improve the positional control of read/write heads for higher density disks is to deploy a voice coil motor (VCM). The deployed VCM is denoted by reference number and is connected to the actuator arm for controlling the motion of the actuator arm and, in turn, controlling a slider of the HGA to position with reference to data tracks across the surface of the magnetic disk, thereby enabling the read/write head imbedded in the slider to read data from or write data to the disk.

Thus, the VCM well performs adjustments to the position of the read/write head. However, as VCM possesses limited bandwidth due to its large inertia, the position control of the read/write head with respect to the track by the VCM has never presented enough accuracy, and thereby the slider cannot reach a quick and fine position control which accordingly affects the ability of the read/write head to read data from and write data to the disk.

In order to solve the problem, dual stage actuator (DSA) has been proposed as one of the alternative methods to increase the servo bandwidth. Piezoelectric material is used in DSA. Piezoelectric rely on the piezoelectric effect, which has two versions. The "direct" piezoelectric effect is the appearance of an electrical potential across certain faces of a crystal when it is subjected to mechanical force. The "reverse" piezoelectric effect, the crystal mechanically distorts in response to application of an electric potential across certain faces of the crystal. DSA is introduced in the hard disk drive in order to modify the displacement of the slider. The hard disk drive employs a dual stage actuator as the additional actuator. The DSA is mounted within the HGA of the disk drive. A piezoelectric based microactuator located on the load beam of the suspension. Specially, the HGA has a suspension to suspend the slider.

It has been a continuing objective of the disk drive industry to produce disk drives of increased storage capacity. One approach to increasing the storage capacity of a hard disk drive is to increase the number of disks. Since data is stored on both sides of the disk therefore it requires two read/write heads per disk. Typically, up to 6 disks are used thus it can be as much as 12 heads and 12 microactuator staked up. Generally, head stack assemblies contain up to 12 head gimbal assemblies which are stacked. However, as the number of disks increases, the physical flexible print circuit size of the drive increases as well. To minimize its occupying area, all dual stage actuators share the same control signal on the flexible printed circuit. As a result, all dual stage actuator circuits are connected in parallel. Since a dual stage actuator can be modeled as a capacitor, the equivalent circuit of dual stage actuator of a head stack assembly is a parallel circuit of capacitors.

As mentioned above, a head stack assembly usually consists of heads, flexures, actuator arms, copper trace, and a flex assembly with a printed circuit board and a preamplifier. Many processing steps are required to manufacture such a

head assembly stack. Each step completed increases the chance that the delicate read/write heads, and dual stage actuator device will be damaged and also improper connectivity. Physical contact between the head and some other mechanical part, for example, improper the connectivity of read/write head and dual stage actuator device. As a result of this improper risk, a manufacturer must verify that the HSA operate properly before placing the head stack assembly into a disk drive. Current dynamic electrical tester (DET) verification methods, although very accurate, dynamic electrical testing is time consuming, expensive, and require space to install.

Another method of testing an HSA is called static testing. In static testing, the DSA of HSA is tested with summation of capacitance. Static testing, although faster, cheaper, and less space is used, has undesirable inherent limitations but it cannot identify which head fail. This is a lack of capability once rework head stack assembly is required. However, conventional methods of testing DSA elements and associated circuitry have not afforded a means for cost effective testing during the manufacturing process. Accordingly, objects of the present invention are to provide an improved system and method for testing HSA's DSA elements and connecting circuitry.

This chapter presents physical product review and current process that has potential to improve testing capability. Analysis of a simple cantilever beam used as a model for actuator arm with PZT element is also explained. According to this model, simulations of the PZT microactuator using finite element method (FEM) were performed. Based on these simulation results, the prototype tester was developed.

3.2 Physical product review

3.2.1 Hard disk drive

Disk drives are widely used in computers and data processing systems for storing information in digital form. These disk drives commonly use one or more rotating storage disks to store data in digital form. Referring to Fig. 3.1, a disk drive includes a drive housing, disk assembly, spindle motor, print circuit board assembly and head stack assembly.

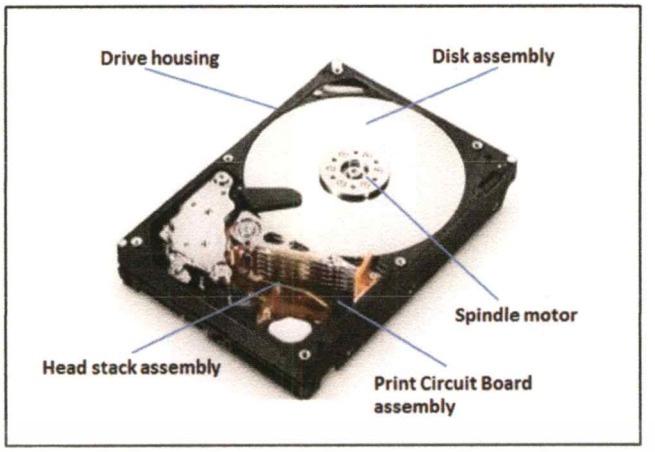

Fig. 3.1 View of hard disk drive

The drive housing retains the various components of the disk drive. The drive housing includes a base and four side walls. A typically drive housing also includes a cover which is spaced apart from the base by the side walls.

The disk assembly includes one or more storage disks that store data in a form that can be subsequently retrieved if necessary. Magnetic storage disks are commonly used to store data in digital form. The magnetic surface of each platter is divided into small sub-micrometer-sized magnetic regions. A typical magnetic region on a storage disk is about 200–250 nanometers wide and extends about 25–30 nanometers in the down-track direction, corresponding to about 100 billion bits per square inch of disk area. The material of the main magnetic medium layer is usually a cobalt-based alloy. Storage disk are typically made using an aluminum or glass substrate.

Depending upon the design of the disk drive, any number of storage disks can be used with the disk drive. Current of disk drive can include one or six storage disks. For two-sided storage disks, the disks are spaced apart a sufficient distance so that at least one transducer assembly can be positioned proximate each of the storage surfaces of adjacent storage disks. To save space, a center line of consecutive disks is typically spaced apart between about one to three millimeters.

The storage disks are spaced apart on a disk spindle which is mounted to a spindle shaft. The spindle shaft is typically secured to the base. The disk spindle rotates on a disk axis relative to the spindle shaft on a spindle bearing assembly.

Typically, the disk spindle and the storage disks are rotated about the disk axis at a predetermined angular velocity by a spindle motor.

3.2.2 Head stack assembly

The head stack assembly is an important part of hard disk drive. The typical HSA has three primary portions: an actuator body that moves in response to the servo control system; head gimbal assembly that extends from the actuator assembly and biases the head towards the disk, and a flexible print circuit that provides an electrical interconnect with minimal constraint on movement.

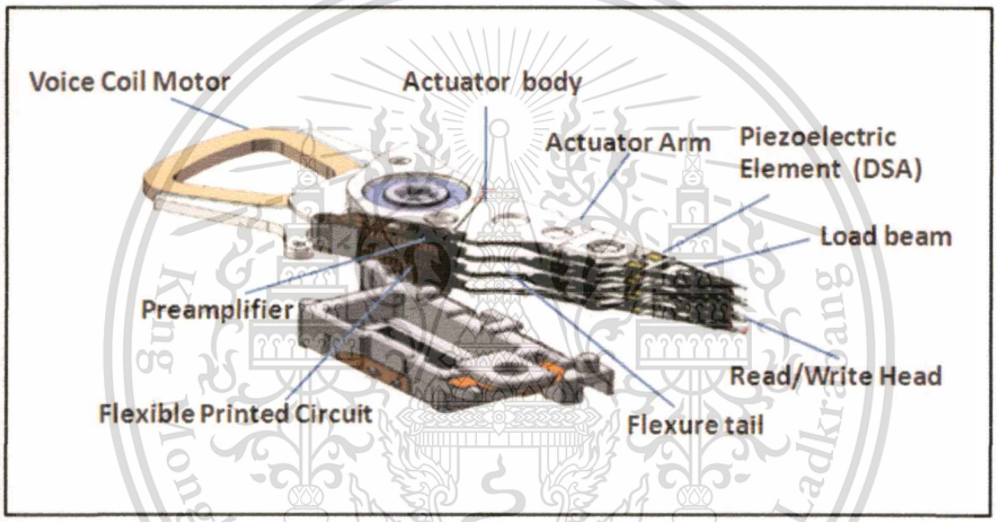

Fig. 3.2 View of head stack assembly

The head stack assembly includes an actuator body and a plurality of actuator arms extending from the actuator body. The actuator body includes a pivot bearing cartridge disposed in the actuator bore, and a voice coil motor that supports a voice coil motor and extends from the actuator body in a direction that is generally opposite the actuator arms. The head stack assembly also includes a plurality of head gimbal assemblies, attached to the actuator arms by swaging. Note that the inner actuator arm includes two head gimbal assemblies, while each of the outer actuator arms includes only one head gimbal assembly. This is because in a fully populated disk drive the inner arms are positioned between disk surfaces while the outer actuator arms are positioned over or under a single disk surface. In a

depopulated disk drive, however, any of the actuator arms may have one or zero head gimbal assemblies, possibly replaced by a balance weight.

The head gimbal assembly is acted as transducer. It transfers information to and from the storage disk. The head gimbal assembly includes a load beam, a flexure, a read/write head secured to the flexure, and a dual stage actuator is nearly secured to the base plate. When the dual stage actuator is energized, the load beam, and thus the read/write head, can be moved back and forth in the tracking direction. Each dual stage actuator independently moves one head gimbal assembly and increases servo band width of hard disk drive. Typically, the dual stage actuator is made from piezoelectric material, ceramic is a part. The load beam attaches the flexure and the slider to the actuator arm. Each load beam is flexible in a direction perpendicular to the storage disk and acts as a spring for supporting the read/write head. Each load beam has a thickness of approximately millimeters scale and is made of full hard stainless steel. Each flexure is used to attach one of the read/write head to one of the load beams. Typically, each flexure includes a plurality of copper traces that are electrically connected to the dual stage actuator and read/write head. Each flexure is subsequently attached to a flex circuit that electrically connects the flexures to the disk drive.

Each head gimbal assemblies includes a head for reading and/or writing to an adjacent disk surface. The head is secured to a tongue portion of a laminated flexure. The laminated flexure is part of the head gimbal assembly, and is attached to a load beam. The laminated flexure may include a structural layer; it makes of stainless steel, a dielectric layer; polyimide is a part, and a conductive layer e.g. copper into which traces are patterned. The head stack assembly also includes a flexible printed circuit adjacent the actuator body, and the flexible printed circuit includes a flex cable. The flexible printed circuit is comprised with a laminate that includes two or more conventional dielectric and conductive layer materials. The laminated flexure includes a flexure tail that includes an intermediate region that is disposed adjacent the actuator arm, and a terminal region that is electrically connected to bond pads of the flexible printed circuit. Methods of electrical connection of the flexure tail to the flexible printed circuit by using an ultrasonic bonding of gold coatings, and anisotropic conductive film bonding.

The flex multiple electrical connection are electrically coupled the dual stage actuator to corresponding flexure tails while multiple electrical connection are electrically coupled the dual stage actuator to corresponding suspension traces. The suspension traces are electrically coupled with a control system which controls the slider as well as the dual stage actuator.

However, as the number of disks increases, the physical flexible print circuit size of the drive increases as well. To minimize its occupying area, all dual stage actuators share the same control signal on the flexible printed circuit. As a result, all dual stage actuator circuits are connected in parallel. Since a dual stage actuator can be modeled as a capacitor, the equivalent circuit of dual stage actuator of a head stack assembly is a parallel circuit of capacitors.

In light of the above, it is an object of this research to provide a head stack assembly having a higher quality. Another object of this research is to detect a defect of dual stage actuator to a traditional head stack assembly with minimal cost to the design of the tester.

In summary, the suspension including read/write head, load beam, piezoelectric element once secured with actuator arm acts as cantilever beam. Lift upward and downward at load beam results in force is applied into piezoelectric element. Therefore, electrical charge can be generated from piezoelectric element. This concept can be used for developing a tester to detect physical conditions of the piezoelectric element. However, to do that is first needs to find a method for applying the controllable force at the load beam while measuring the electrical signal from the piezoelectric element in response to that force. This method must not cause any damages on the HSA and must be practical for production line. A possible solution is to adapt an existing technique that is currently used in the gram load tester implemented in the production line.

3.2.3 Gram load machine

In current head stack assembly manufacturing, a known system for measuring spring characteristic of the load beam of the head gimbal assembly is called gram load tester. It uses to verify gram load of head stack assembly before installing in hard disk drive. The gram load tester includes a computer for storing gram load measurements, a gram load measuring instrument, and the nest for placing each of

the suspension arms of a head stack assembly into position to measure the gram load. Figure 3.3 illustrates the nest for placing each of the suspension arms of a head stack assembly into position to measure the gram load. The nest includes a spreader pin tower assembly comprising a plurality of vertically aligned spreader pins for mesh engaging suspension arms such as those of the head stack assembly. As the spreader pins and the suspension arms engage each spreader pin is placed between a top and bottom arm. Each spreader pin includes an L-shaped lever arm integrally press-fit at one end. In spreader pin tower, the incrementally varying lengths of the pins form a step-like staggered array of levers, enabling each to be rotated without interference from adjacent levers. To measure the gram load of each arm, each lever arm had to be rotated. For example, to measure a gram load of the first head (i.e. the bottom one in Fig. 3.3), the first lever is first rotated 90 degrees in the clockwise direction, releasing the first suspension arm in contact with a disk simulator which prevented adjacent heads from contacting each other as illustrated in Fig. 3.4. Accordingly, the tester would prompt the measuring of the gram load of the bottom suspension arm. Then, the pin lever is again manually rotated 180 degrees in the other direction, returning the first suspension arm to its original position, and releasing the second suspension arm in contact with the adjacent disk simulator as shown in Fig. 3.5. Again the operator is require to prompt the measuring of the gram load of the top suspension arm. This process of rotating the pin lever arm, then prompting the measuring gram load is repeated until the gram load in every suspension arm is measured.

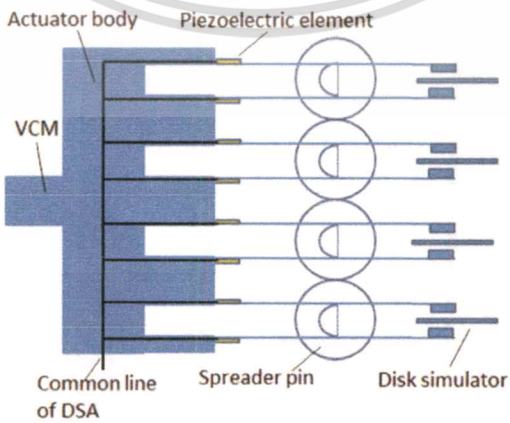

Fig. 3.3 The nest for placing each of the suspension arms of a head stack assembly into position to measure the gram load

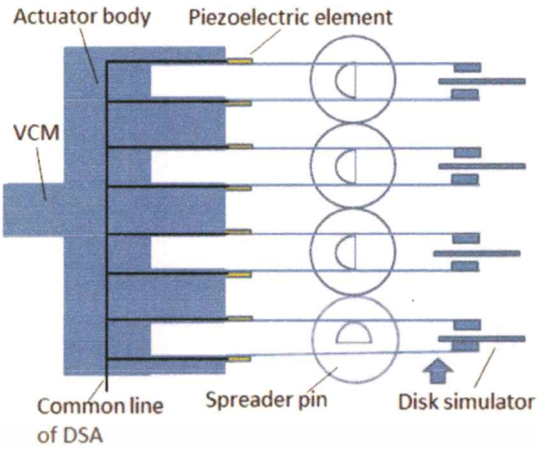

Fig. 3.4 The nest for placing each of the suspension arms of a head stack assembly into position to measure the gram load for bottom head

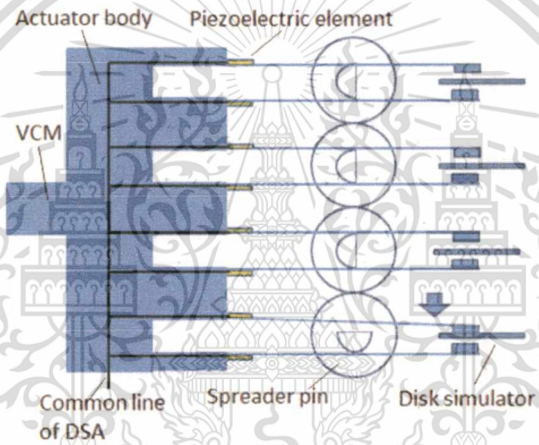

Fig. 3.5 The nest for placing each of the suspension arms of a head stack assembly into position to measure the gram load for top head

Clearly the advantage of this system is the moving upward and downward of suspension arm of particular head individually with controllable of spreader pin. This process can generate force to suspension arm and stress/strain is occurred in suspension. The spreader pin tower assembly allows force to be applied to each suspension arm sequentially without interference between each other. During releasing head contact with disk simulator. Force is generated in load beam resulting in stress/strain on the piezoelectric element. Piezoelectric element will then generate electrical charge which is detectable as an electrical signal. When the piezoelectric elements with different physical conditions are subject to the same stress/strain, they create different electrical signals. Consequently, this technique of

measuring gram load can be adapted for non-functional dual stage actuator detection.

3.2.4 Concept of detector for non-functional DSA

The dual stage actuator is designed and operates based on the reverse piezoelectric effect. In its operation, the appropriate control signal is applied to the electrodes of PZT and produces some deformation of the PZT element on the x-y plane as illustrated in Fig. 3.6. The deformation causes a micro-scale displacement on the read/write head. During the read/write access, the off-track error is used as a feedback signal to form a closed-loop control system which maintains read/write head at its correct position on the track. According to the direct piezoelectric effect as described in chapter 2, stress/strain on the PZT element can result in voltage difference between its electrodes. Therefore if a certain amount of external force is applied to the PZT element, electrical signal from its electrodes will be generated and be detectable. Considering the structure of head stack assembly and its PZT, it is found that a controllable force can be exerted individually on each suspension arm in the z direction. This will create stress/strain only on the PZT element mounted on that actuator arm. Thus electrical signal corresponding to that particular PZT can be observed at the same terminal which is connected to the control signal. The characteristic of this signal can provide information about conditions of PZT element and its circuit connectivity.

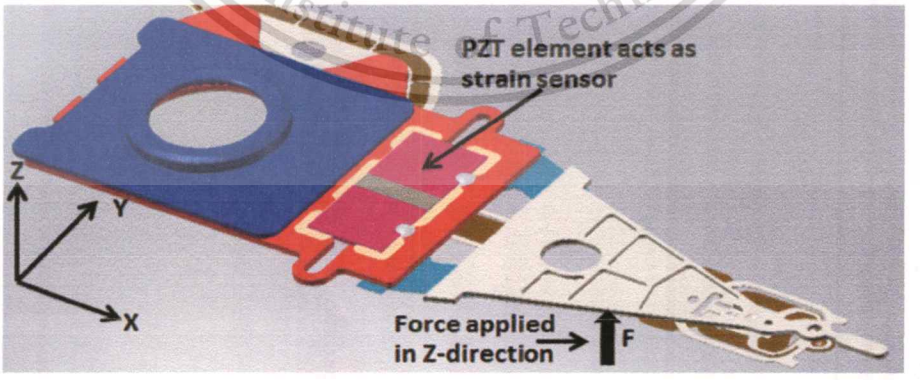

Fig. 3.6 Piezoelectric element on suspension arm and the reference axis for apply force and its deformation

3.3 Analysis and simulation of a simple cantilever beam with the PZT microactuator

In order to gain insight into the concept of the non-function DSA detector, the suspension arm with piezoelectric element is modeled as a cantilever beam. Once force is applied at the free-end of the beam perpendicularly to the beam axis, it would bend and cause stress/strain on the beam including the piezoelectric element. This defection and stress/strain can be analyzed using classical mechanic as follows.

3.3.1 Cantilever beam – Beam stiffness [14]

There is a linear relationship between the force and deflection of a cantilever beam, as long as the deflection is small and the beam material does not yield. It is also expressed as force per unit distance. For a deflection at the end of the beam perpendicular to the beam axis, the force can be expressed as:

$$F = \left\lfloor \frac{3 . E . I}{L^3} \right\rfloor . d \tag{3.1}$$

Here, **E** is the elastic modulus of the material, **I** is the area moment of inertia of the beam cross section, and **L** is the length of the beam. Note that the stiffness depends on the geometry of the beam as well as the material stiffness of the beam. For a straight beam with a rectangular cross section, the moment of inertia of the beam, which is a measure of how the cross-sectional area is distributed around its center, it can be calculated as:

$$I = \frac{1}{12} . w . t^3 \tag{3.2}$$

Here, **w** is the strip width and **t** is the strip thickness. Therefore, the force generated by a given deflection is

$$F = \left\lfloor \frac{E.w.t^3}{4.L^3} \right\rfloor . d \tag{3.3}$$

The stiffness of the beam is thus given by the bracketed term in the eq. (3.3). Note that the overall stiffness is a function of the elastic modulus (material stiffness) and the dimensions of the beam (geometric stiffness.) Note that this equation is only valid if the stress in the spring does not exceed the elastic limit of the metal. If the material should start to yield, the elastic modulus is no longer a constant, and the equation will predict a value for force that is much greater than what it is in reality. The cantilever beam is illustrated as Fig. 3.7.

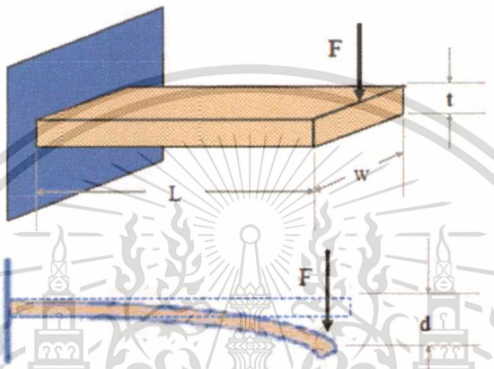

Fig. 3.7 Cantilever beam

In a cantilever beam under a bending load, the stress is different at every point in the beam. When a beam is bent downward, the top surface of the beam elongates and is in tension. The bottom surface becomes compressed. Somewhere near the center of the beam, there is a plane that neither elongates nor compresses and thus is under no stress. This is known as the neutral axis. The stress will increase from zero at the neutral axis to a maximum value at the upper and lower surfaces, as shown in Fig. 3.8.

The stress will vary along the length of the beam, as well as through the thickness. The stress at any point depends on the bending moment (torque) present at that point. The bending moment (M) at any point in the beam is equal to the force applied multiplied by the distance from that point to the point of application. It is therefore zero at the free end of the beam, and maximum at the fixed end. This means that there is no stress at the free end of the beam, and a maximum stress at the fixed end. The equation for the stress at any point in the beam is as follows:

$$\text{Stress} = \sigma = \frac{M.y}{I} = \frac{F.x}{I}.y \tag{3.4}$$

Here, **F** is the force applied, **x** is the distance from the point of force application, I is the moment of inertia, and **y** is the distance from the neutral axis.

There are some interesting consequences of these equations. Notice that the width of the beam affects the contact force but has no effect on the stress. The contact force is most influenced by thickness and length, while the stress is most influenced by length. Both the stress and force are linearly proportional to the elastic modulus and the deflection.

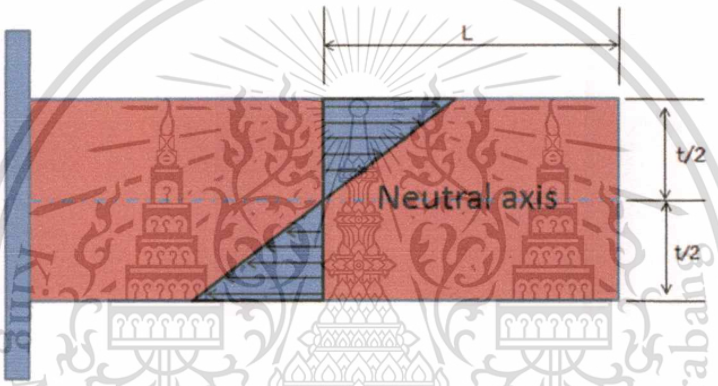

Fig. 3.8 Cantilever beam strain distribution

3.3.2 Simulation setup and data analysis

As disk drives become ever smaller, the suspension holding the read/write head becomes a larger portion of the actuator assembly and plays a more important role in the overall dynamics of the system. In order to gain a better understanding of the computer simulation can be very useful. With such a tool, parametric studies can be easily performed and assumptions about the suspension's behavior can be validated.

In this study, finite element analyses are performed using the software ANSYS. The simulation and data analysis is performed based on Western Digital suspension design.

The simulation setup and data analysis are as follows:

1. Create the suspension model with normal PZT element per Western Digital design.

2. Vary displacement downward by -0.5, -1.0, -1.5 and -2.0 mm. respectively. In each displacement step stress and strain on the PZT element are recorded simultaneously at 5 different locations as shown in Fig. 3.10
3. Vary displacement upward by 0.5, 1.0, 1.5 and 2.0 mm. respectively. In each displacement step stress and strain on the PZT element are recorded simultaneously at 5 different locations as in step 2
4. Repeat step 1 – step 3 but use the suspension model with cracked PZT element
5. Compare stress and strain each point between the normal and the cracked PZT element.

The suspension model for finite element method is shown in Fig. 3.9 and stress and strain are measured in 5 different areas as shown in Fig. 3.10. The finite element simulation includes model and material parameter setup as listed in Table 3.1.

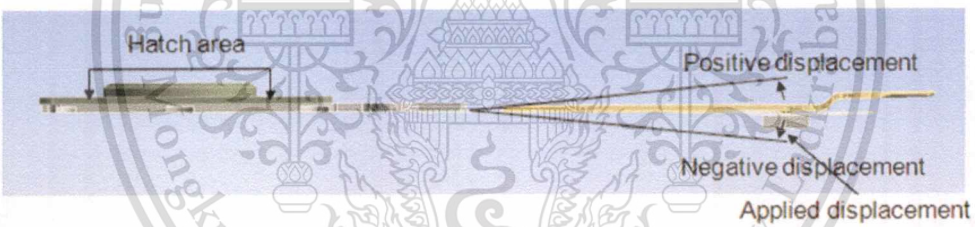

Fig. 3.9 View of the finite element model used for stress/strain simulation of head gimbal assembly secured with actuator arm

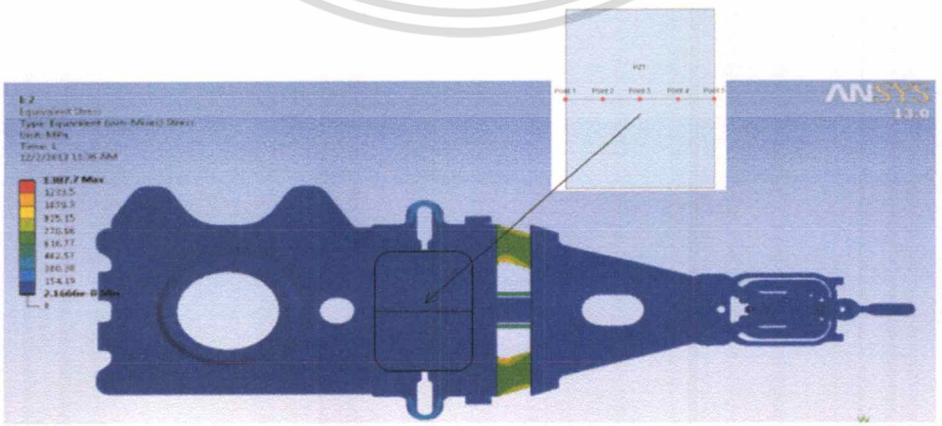

Fig. 3.10 Position to observe stress/strain

Table 3.1 Mechanical properties of suspensions

Component	Thickness (mm)	Young's modulus (Pa)	Poisson's ratio
Base plate	Confidential	Confidential	Confidential
Load beam	Confidential	Confidential	Confidential
Stiffness	Confidential	Confidential	Confidential
Flex SST	Confidential	Confidential	Confidential
Flex PI	Confidential	Confidential	Confidential
Flex CU	Confidential	Confidential	Confidential
PZT	Confidential	Confidential	Confidential

The relation of stress/strain and displacement of the normal and cracked PZT is obtained by finite element analyses. Figure 3.11 shows stress on suspension with normal PZT when driven at 2.0 mm. Figure 3.12 and Figure 3.13 show plots of stress and strain on suspension with normal PZT when driven at different displacement. To simplify the plots, each data point represents the average of stress and strain simulated from 5 locations. The results show that for the normal PZT stress and strain increase linearly as the displacement increase. They also appear to be symmetric to the both directions of the displacement. The plots of stress and strain on a suspension with cracked PZT are shown in Fig. 3.14 and Fig. 3.15 respectively. In this case, the simulated stress and strain are not symmetric, much lower in amplitude, less linear than that of the normal PZT. To display their dissimilarity, both simulation results are plotted in Fig. 3.16 and Fig. 3.17. According to these results, it can be concluded that there is a significant distinction of stress and strain occurred on suspensions with a normal PZT and a cracked PZT.

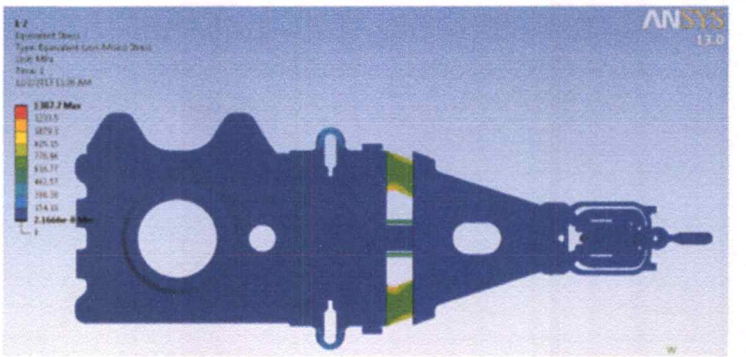

Fig. 3.11 Stress on suspension with normal PZT at -2.0 mm displacement

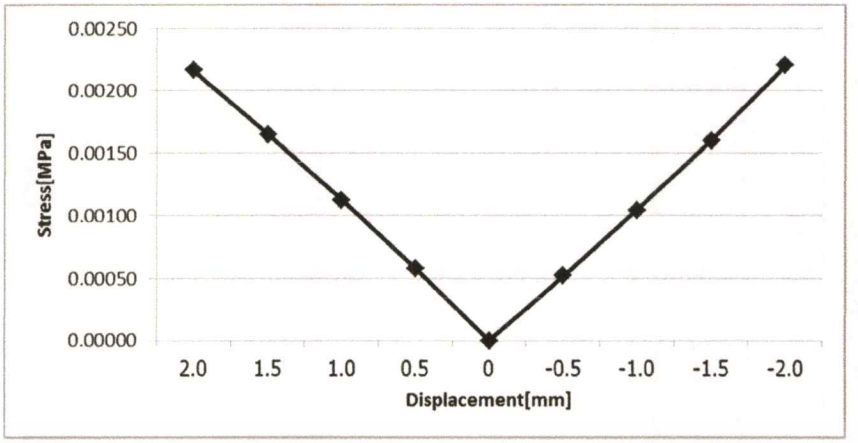

Fig. 3.12 Stress on suspension with normal PZT

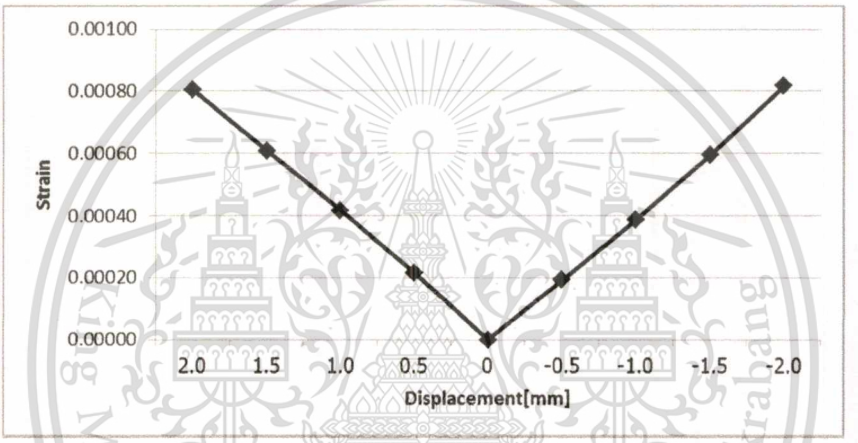

Fig. 3.13 Strain on suspension with normal PZT

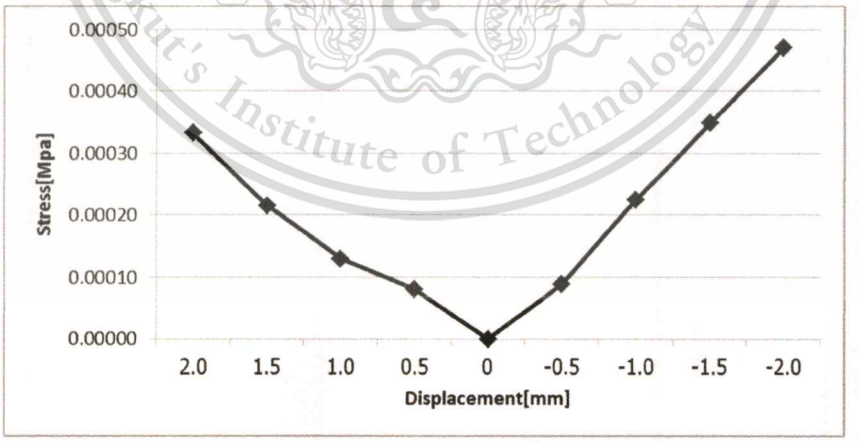

Fig. 3.14 Stress on suspension with cracked PZT

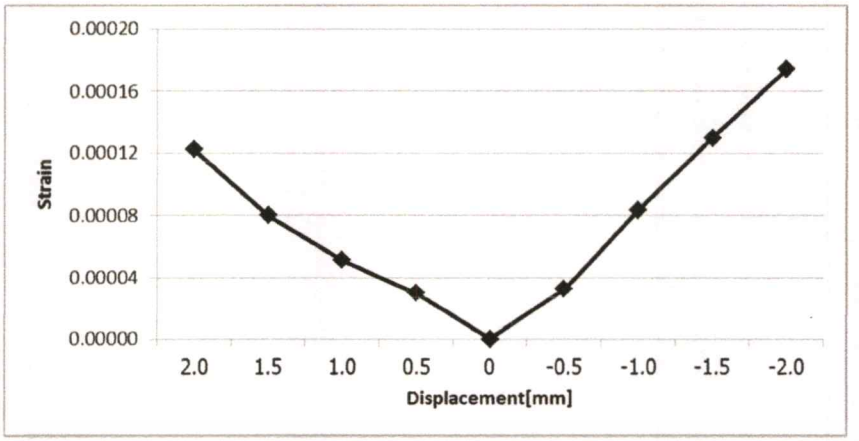

Fig. 3.15 Strain on suspension with cracked PZT

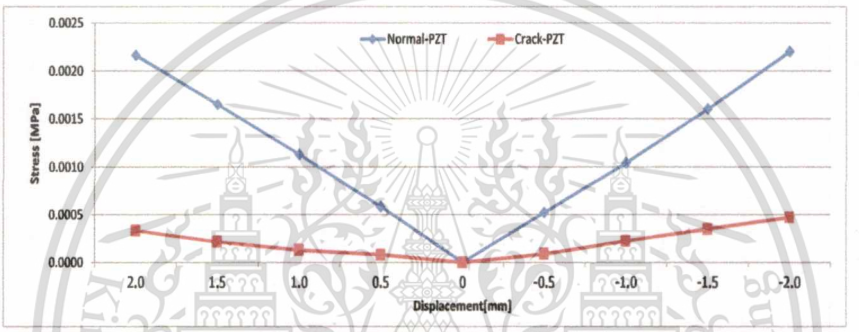

Fig. 3.16 Stress comparisons between normal and cracked PZT

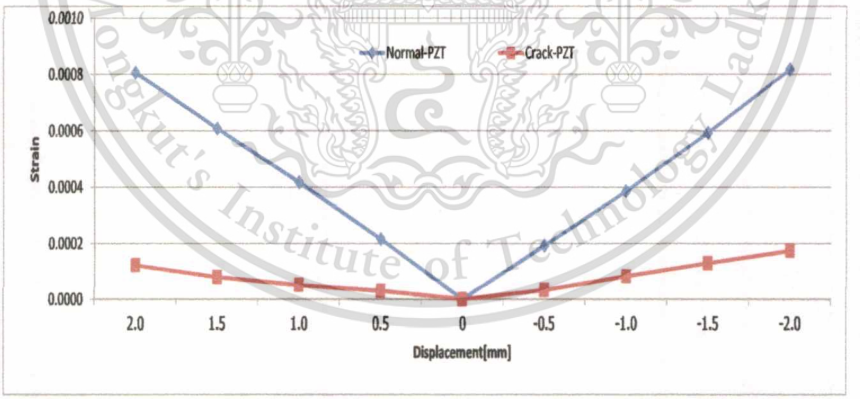

Fig. 3.17 Strain comparisons between normal and cracked PZT

Refer to the model, the dual stage actuator made from piezoelectric material. It is secured into suspension. The suspension is secured to actuator arm by swaging. Therefore, it is acted as a cantilever beam. Once displacement is created at the distal end, there is stress/strain occurred at dual stage actuator element. From this occurrence, it can be predict that moving upward and downward at gram load tester

can develop stress/strain at dual stage actuator. Since, the dual stage actuator is made from piezoelectric material. It will generate the electrical signal.

3.4 Tester development

Since the head stack assembly includes 3 primary portions. They are an actuator body that moves in response to the servo control system; head gimbal assembly that extends from the actuator arm assembly and biases the head towards the disk and a flexible print circuit that provides an electrical interconnect with minimal constraint on movement. In the new design of head gimbal assembly is integrated to the dual stage actuator at near baseplate. In each particular actuator arm, a read/write head is mounted at the distal end of each of the actuator arm by swaging. It is act as cantilever beam. From simulation results, applying the force at the end of the cantilever beam, create stress/strain at dual stage actuator area. With this head stack assembly design, concept of using gram load tester to apply amount of controllable mechanical force to the head suspension to excite its piezoelectric element can be realized. Once the piezoelectric element is excited, the electrical signal corresponding to its physical condition whether it is normal or cracked can be monitored. Based on this approach, a tester to characterize dual stage actuator can be developed.

Figure 3.18 shows a novel dual stage actuator measuring system. It has been designed according to the principle explained in previous section. Since it is intended to be used as standard equipment in the production line, it must be easy to operate and consume short operating time. The system included a front-end fixture which is designed for placing each of the suspension arm of a head stack assembly into position to measure the dual stage actuator and applying a controllable force to a load beam of the selected read/write head individually, a data acquisition and signal processing unit, and a computer for store and display the measurement result.

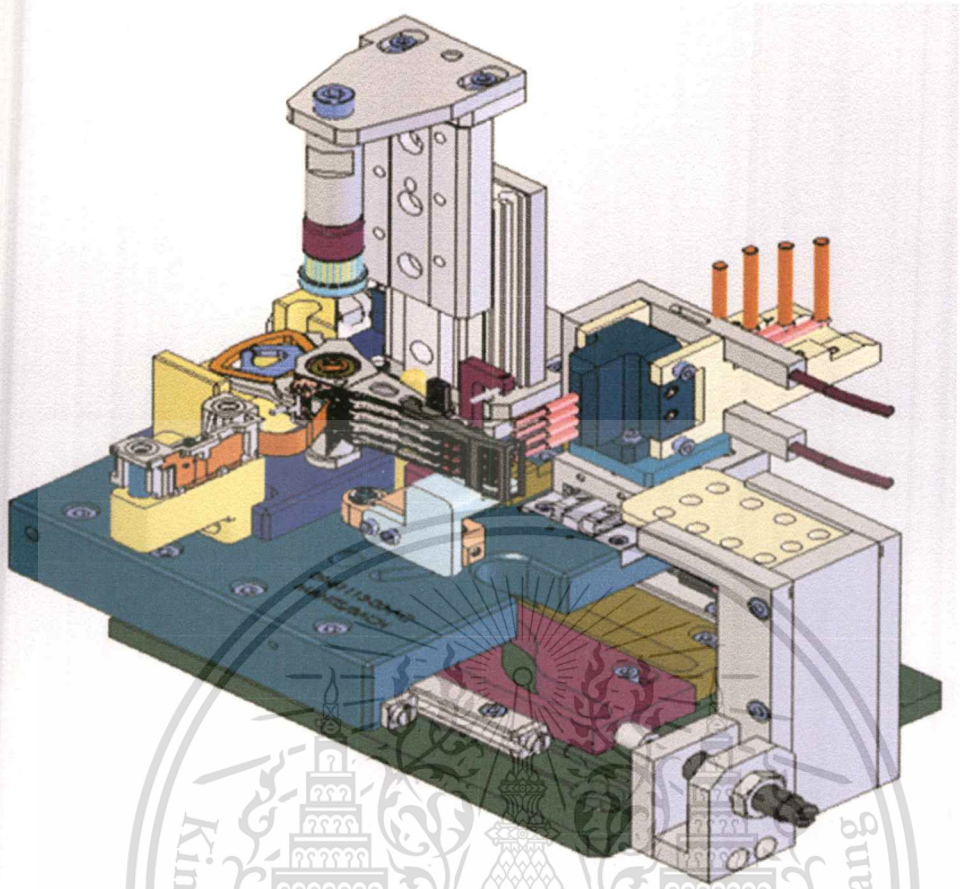

Fig. 3.18 Perspective view of the tester loaded with a head stack assembly

3.4.1 Operation of the tester

The operation of the tester can be described as follows. After loading, signal from flexible printed circuit of head stack assembly are then connected to the data acquisition and signal processing unit. In this part, the analog signal generated by the PZT due to deflection of load beam is amplified and converted to digital for further processing. Signal characteristics including shape and its amplitude are recorded and displayed on the data screen. This procedure continues on each head individually until complete all heads. Diagram shows the operation of the tester us depicted in Fig. 3.19.

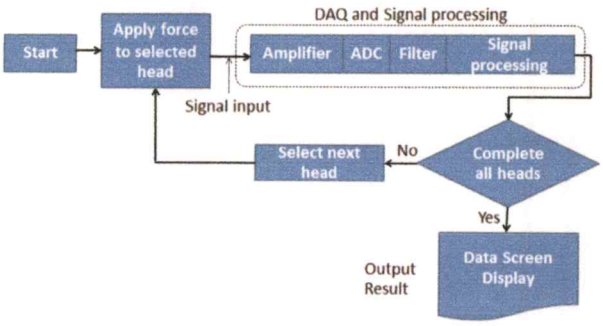

Fig. 3.19 Block diagram of the tester operation

Figure 3.20 illustrates the apparatus, including a spreader pin tower assembly comprising a plurality of vertically aligned spreader pin for mesh engaging suspension arm such as those of the head stack assembly. Each spreader pin includes an L-shaped lever arm integrally press-fit at one end as show in Fig. 3.21.

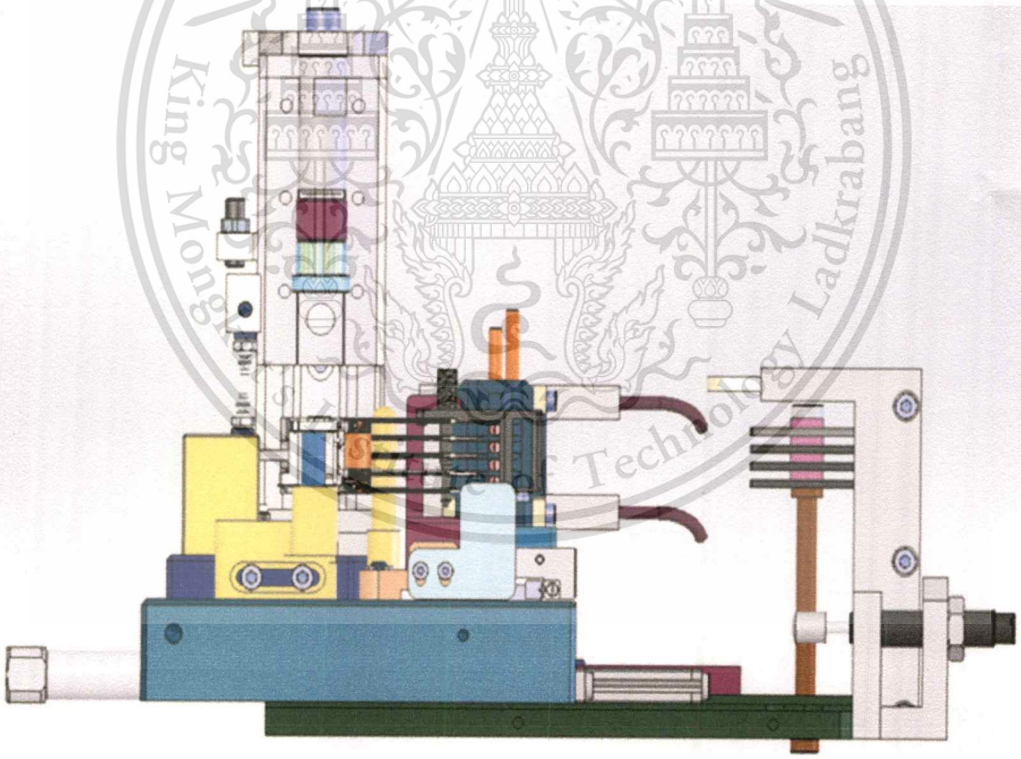

Fig. 3.20 Side view of the tester shows spreader pin tower assembly

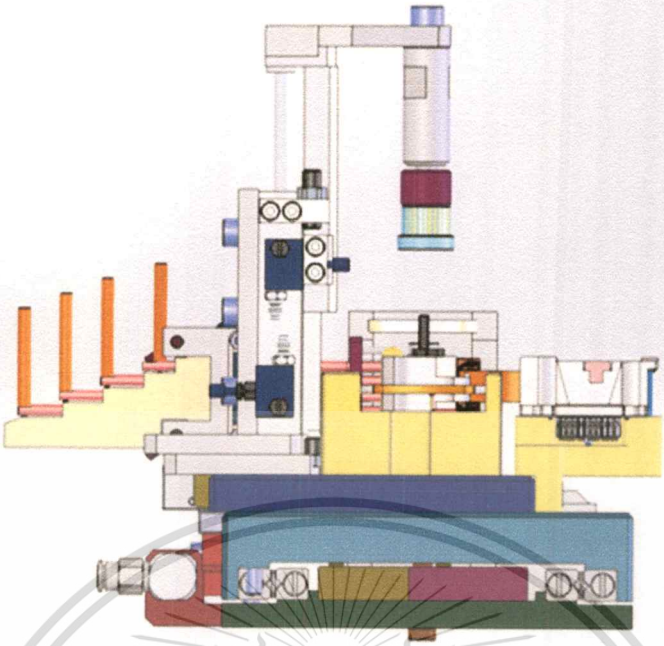

Fig. 3.21 Side view of the tester shows L-shaped lever arm

As the spreader pins and the suspension arms engage, shown in Fig. 3.22, each spreader pin is situated between a top and bottom actuator arm. Each spreader pin includes an L-shaped lever arm integrally press-fit at one end. The incrementally varying lengths of the pins form a step-like staggered array of levers, enabling each to be rotated without interference from adjacent levers. To measure the dual stage actuator of each arm, each lever arm had to be rotated. For example, each lever was first manually rotated 90 degrees in the clockwise direction, releasing the bottom suspension arm in freely state angle, shown in Fig. 3.23 which prevented adjacent heads from contacting each other. Then, the spreader pin lever is again manually rotated 180 degrees in the other direction, returning the bottom suspension arm to its original position, shown in Fig. 3.24, and releasing the top suspension arm in freely angle. This process of manually rotating the lever arm, then prompting the measuring apparatus and the computer is repeated until the dual stage actuator in every suspension arm is measured. Figure 3.25 and Figure 3.26 illustrate examples of a screen capture of the test result. It shows normalized signals measured from DSA. Notice that amplitudes of the signals from heads with cracked PZT element are much smaller than that with the normal PZT element.

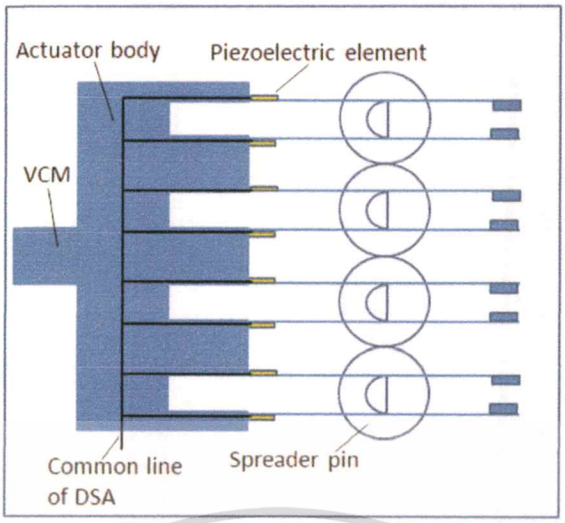

Fig. 3.22 Each spreader pin is situated between a top and bottom actuator arm

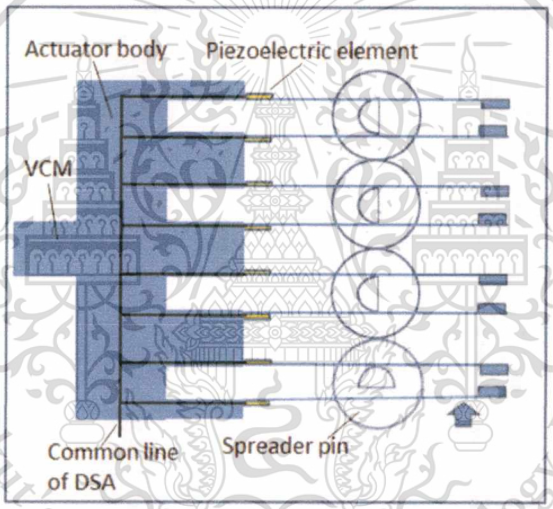

Fig. 3.23 Spreader pin is rotated to measure bottom head

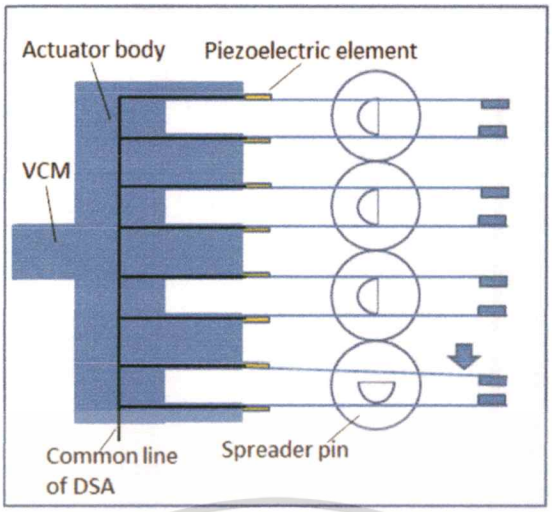

Fig. 3.24 Spreader pin is rotated to measure top head

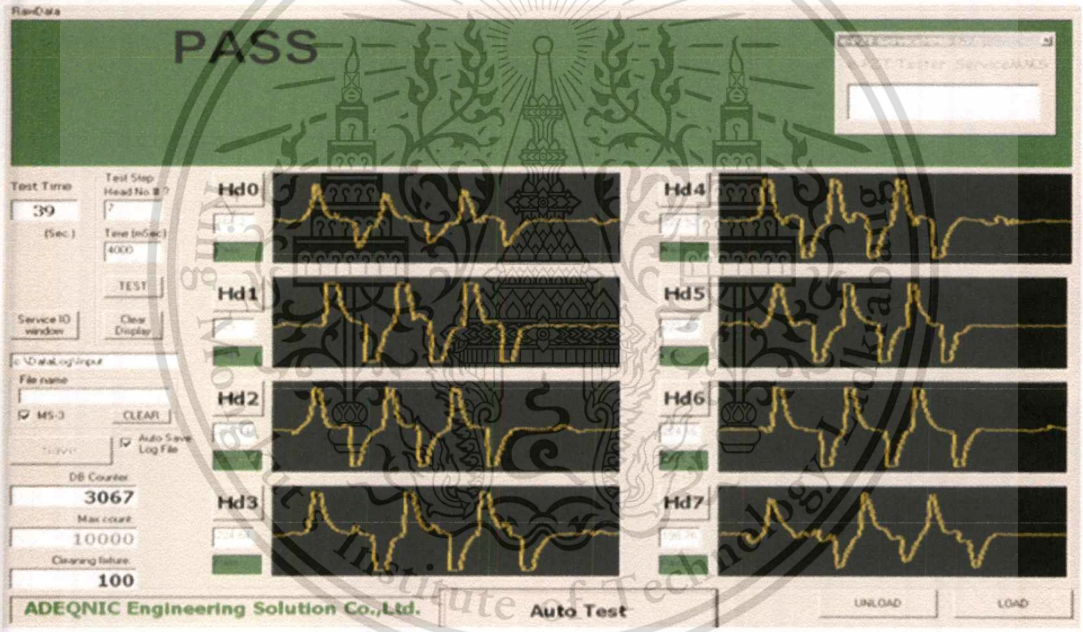

Fig. 3.25 Test "Pass" results from the system

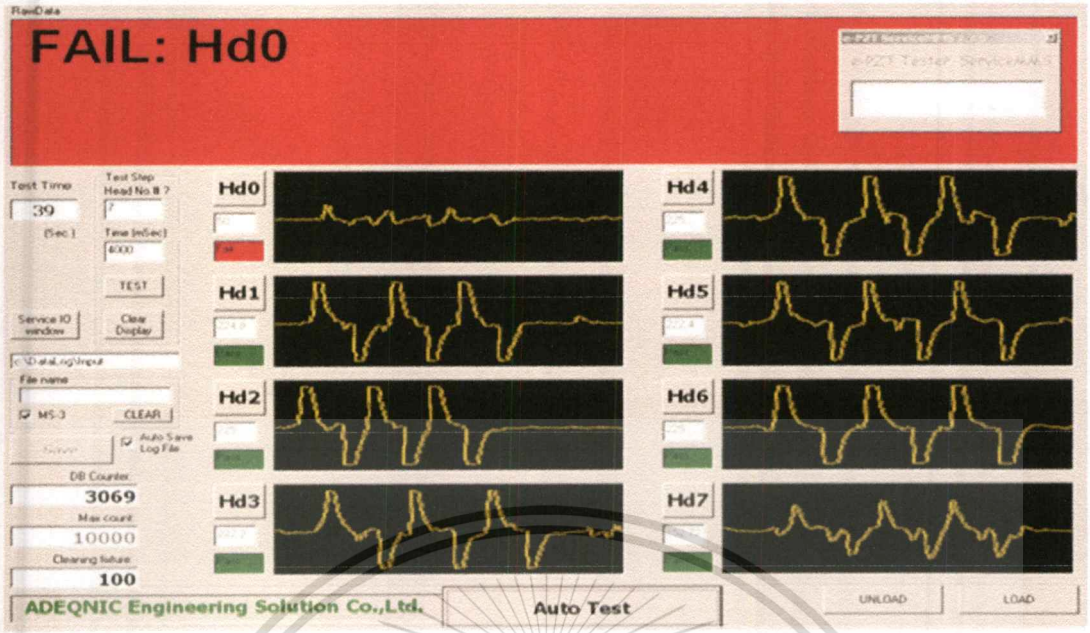

Fig. 3.26 Test "Fail" results from the system

3.5 Summary

In this chapter the concept of testing non-functional DSA using the reverse piezoelectric effect has been described. That is applying force to the actuator suspension arm to create stress and strain on PZT element of the actuator. This, in turn produces electrical signal to the input of the actuator circuit. The difference in electrical signal generated by the PZT element is then used to identify whether the PZT is normal or cracked. To verify this concept, a head gimbal assembly was first modeled and simulated as a cantilever beam experiencing external force and causing stress and strain on the PZT element. The model and the simulation were performed using a commercial software ANSYS. The simulation results show that it is possible to use the electrical signal from PZT to identify its physical condition. To implement the tester based on this concept, a technique which currently used in gram load tester was reviewed and adapted to use in this newly design tester. This technique allows a controllable force to be applied to each head of the HSA individually. As results, the novel tester has been developed. It is capable of identify which head of the HSA has a non-functional DSA due to either defects of its connectivity or the cracked PZT.

Chapter 4
Experimental Results

4.1 Introduction

In previous chapter, the design concept and the development of the dual stage actuator measurement system has been explained. The prototype system which from now will be called the ePZT is based upon the recognition that a wide range of dual stage actuator failure modes can be efficiently detected by causing relative movement between suspension portions being driven with respect to dual stage actuator, and monitoring and evaluating the electrical signals produced by the dual stage actuator. The signals from the actuator having a failure mode are sufficiently different than those of a properly functioning actuator. Therefore, the operational state of the actuator can be accurately assessed.

Next step, to ensure that the ePZT is suitable for implementation in a production line, it needs to pass qualification process. To qualify the ePZT, extensive testings were performed. The procedure and their test results are subject to this chapter.

4.2 Testing Parameter

To evaluate its performance, ePZT was first tested using HSA with three kinds of condition; HSA with good PZT element, HSA with damaged PZT element (or micro crack) as shown in Fig. 4.1 and HSA with the open-circuit actuator. The waveforms of signals measured from its actuator circuit are shown in Fig. 4.2. It can be observed that signals from both good and cracked PZT have a similar shape but different amplitudes. Its positive and negative amplitude are corresponding to the deflecting up and down of the load beam during applying a controllable force. Note that in case of the good PZT element its signal amplitude are noticeable larger than the cracked PZT. For the case of an open circuit, there is no waveform generated.

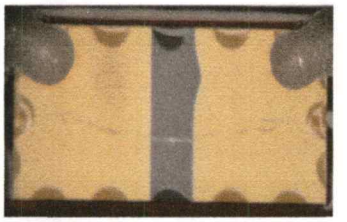

Fig. 4.1 Microphotograph of the damage PZT element due to crack across from left to right

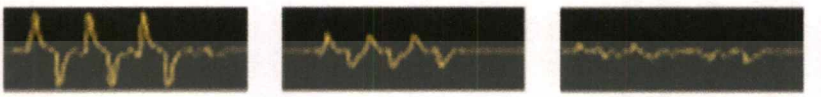

(a) (b) (c)

Fig. 4.2 Waveform of signals measured from PZT actuator circuits by ePZT: (a) a good PZT element, (b) a PZT element with crack, and (c) an open circuit actuator circuit

Based on this preliminary measurement results, the quantity that implies conditions of PZT elements is the amplitude of the signal, therefore three amplitude-related parameters are defined and recorded for the analysis as follows.

Amplitude_Max: The positive peak voltage of the signal.

Amplitude_Min: The negative peak voltage of the signal.

RMS_Amplitude: The root mean square of the signal which is defined as

$$RMS\_Amplitude = \sqrt{\frac{1}{n}\sum_{i=1}^{n} V_i^2} \quad \text{where } i = 1,2,3...,n$$

Note that the reference level of the signal is the voltage level measured when there is no force applied. In this case it is set to be zero volt. These definitions are illustrated in Fig. 4.3.

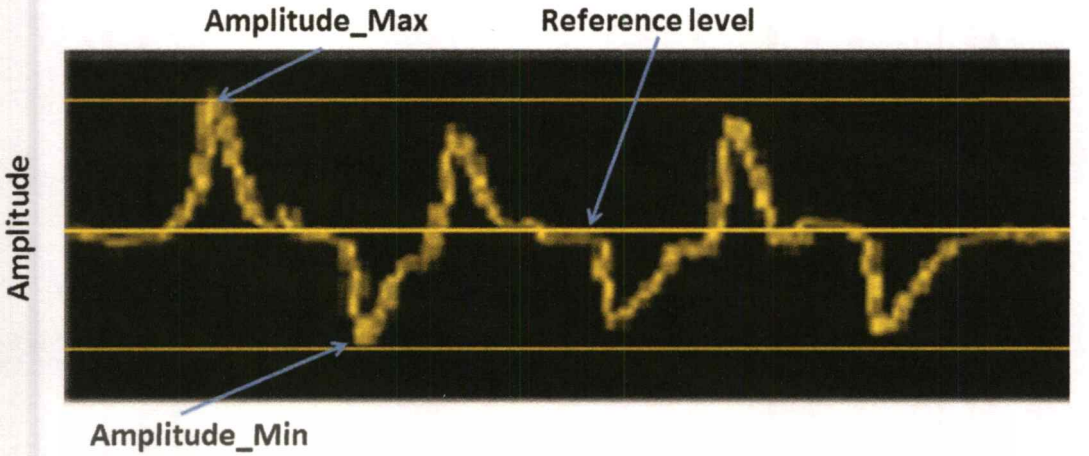

Fig. 4.3 The measured signal from ePZT and its parameter definition

Because the waveform shows approximately the same value for positive and negative amplitude, thus for simplicity, only Amplitude_Max is chosen to use in statistical analysis. At the moment, the RMS value is used for comparison its electrical response particularly among the good PZT elements.

4.3 Testing Procedure

There are two possible failure modes found in the non-functional DSA. The first one are defects in DSA circuit connectivity. It can be an open circuit of DSA control path due to open bonding, broken wires, and discontinuity of flexure traces. The second type of failure is due to defects of PZT element, particularly, a cracked PZT. In the standard procedure, there are two methods to identify those failures, a visual inspection and a stoke test using dynamic electrical test (DET). Testing and characterization using DET is considered as the reference to classify whether or not the DSA is functional and qualified. Therefore, in this experiment a fairly large amount of samples from HSA production line were tested using ePZT and then compared with test results from both visual inspection and DET. An example of test result comparison between ePZT, DET and visual inspection is shown in Table 4.1.

Table 4.1 Example of the test results shows performance comparison between the dual stage actuator measurement system (ePZT) and dynamic electrical test (DET)

Head	Part ID	Amplitude_max_ePZT	Stroke_DET (uIn)	Visual	Head	Part ID	Amplitude_max_ePZT	Stroke_DET (uIn)	Visual
Hd 0	FTDLMHZL569	86.551	22.578		Hd 0	FTDLQHUG0Q9	62.615	15.167	
Hd 1	FTDLMHZL569	80.129	22.454		Hd 1	FTDLQHUG0Q9	69.203	23.363	
Hd 2	FTDLMHZL569	106.113	22.876		Hd 2	FTDLQHUG0Q9	98.954	22.599	
Hd 3	FTDLMHZL569	88.402	21.185		Hd 3	FTDLQHUG0Q9	21.351	11.533	Crack
Hd 4	FTDLMHZL569	15.985	0.000	Open Bonding	Hd 4	FTDLQHUG0Q9	44.354	22.362	
Hd 5	FTDLMHZL569	13.061	0.000	Open Bonding	Hd 5	FTDLQHUG0Q9	47.859	23.096	
Hd 6	FTDLMHZL569	89.804	21.197		Hd 6	FTDLQHUG0Q9	34.382	23.622	
Hd 7	FTDLMHZL569	66.318	22.834		Hd 7	FTDLQHUG0Q9	30.293	22.912	
Hd 0	FTDLPHYWF49	50.795	24.567		Hd 0	FTDLQQZZE69	15.887	0.000	Crack
Hd 1	FTDLPHYWF49	88.615	20.319		Hd 1	FTDLQQZZE69	112.155	22.211	
Hd 2	FTDLPHYWF49	80.689	23.131		Hd 2	FTDLQQZZE69	98.145	21.948	
Hd 3	FTDLPHYWF49	93.176	20.526		Hd 3	FTDLQQZZE69	62.687	22.541	
Hd 4	FTDLPHYWF49	71.387	23.626		Hd 4	FTDLQQZZE69	75.705	23.235	
Hd 5	FTDLPHYWF49	79.019	21.451		Hd 5	FTDLQQZZE69	115.366	22.101	
Hd 6	FTDLPHYWF49	21.079	0.000	Open Bonding	Hd 6	FTDLQQZZE69	142.522	20.451	
Hd 7	FTDLPHYWF49	67.044	21.530		Hd 7	FTDLQQZZE69	40.602	23.129	
Hd 0	FTDLPN2JC39	74.717	22.121		Hd 0	FTDLR31NM99	51.925	22.161	
Hd 1	FTDLPN2JC39	79.658	21.308		Hd 1	FTDLR31NM99	87.009	21.135	
Hd 2	FTDLPN2JC39	117.579	22.255		Hd 2	FTDLR31NM99	55.564	22.725	
Hd 3	FTDLPN2JC39	81.287	21.785		Hd 3	FTDLR31NM99	86.589	22.203	
Hd 4	FTDLPN2JC39	5.050	0.000	Open Bonding	Hd 4	FTDLR31NM99	44.847	23.464	
Hd 5	FTDLPN2JC39	106.920	21.325		Hd 5	FTDLR31NM99	72.744	22.085	
Hd 6	FTDLPN2JC39	111.713	21.461		Hd 6	FTDLR31NM99	24.377	18.664	Crack
Hd 7	FTDLPN2JC39	68.965	22.266		Hd 7	FTDLR31NM99	69.054	23.247	
Hd 0	FTDLQ8WSE89	93.566	22.301		Hd 0	FTDLR9QMBH9	5.555	0.000	Open Bonding
Hd 1	FTDLQ8WSE89	138.176	19.728		Hd 1	FTDLR9QMBH9	84.029	22.162	
Hd 2	FTDLQ8WSE89	84.048	21.393		Hd 2	FTDLR9QMBH9	90.103	22.100	
Hd 3	FTDLQ8WSE89	131.518	19.338		Hd 3	FTDLR9QMBH9	63.776	21.852	
Hd 4	FTDLQ8WSE89	120.456	21.791		Hd 4	FTDLR9QMBH9	95.183	22.714	
Hd 5	FTDLQ8WSE89	93.300	21.731		Hd 5	FTDLR9QMBH9	72.606	22.366	
Hd 6	FTDLQ8WSE89	15.550	0.000	Open Bonding	Hd 6	FTDLR9QMBH9	94.686	23.496	
Hd 7	FTDLQ8WSE89	50.277	22.027		Hd 7	FTDLR9QMBH9	38.857	21.891	
Hd 0	FTDLQFUFMS9	15.275	0.000	Open Bonding	Hd 0	FTDLR9VMBE9	61.063	22.402	
Hd 1	FTDLQFUFMS9	70.349	21.660		Hd 1	FTDLR9VMBE9	69.893	23.150	
Hd 2	FTDLQFUFMS9	38.538	17.225	Crack	Hd 2	FTDLR9VMBE9	89.296	22.255	
Hd 3	FTDLQFUFMS9	60.878	22.332		Hd 3	FTDLR9VMBE9	5.050	0.000	Open Bonding
Hd 4	FTDLQFUFMS9	75.773	21.350		Hd 4	FTDLR9VMBE9	70.618	22.392	
Hd 5	FTDLQFUFMS9	59.281	22.608		Hd 5	FTDLR9VMBE9	66.663	22.211	
Hd 6	FTDLQFUFMS9	70.931	22.032		Hd 6	FTDLR9VMBE9	78.632	23.424	
Hd 7	FTDLQFUFMS9	54.506	21.316		Hd 7	FTDLR9VMBE9	43.343	22.334	

According to the table, the test results are of HSAs with eight heads i.e. eight DSA. It appears that a DSA with cracked PZT element produces a signal to ePZT with significantly lower in amplitude than a DSA with a normal PZT element. Correspondingly, the displacement of that DSA measured with DET is noticeably lower than average. For a DSA with an open bonding, there is no measurable displacement from DET since biasing signal cannot reach or partially reach the PZT. However, in this case, very small signal amplitude from ePZT is detected. This is possibly due to two reasons. Firstly, the open bonding does not mean completely open circuit. It means that there is a certain amount of resistance greater than a specific pre-defined value appeared in the circuit path such as a large resistance from a broken wire bond. Secondly, it is due to fact that the displacement of suspension causing stress/strain in ePZT measurement is in the direction perpendicular to the displacement of PZT element due to DET. As a result, the responses of PZT element are different.

From the comparison, it shows good agreement between ePZT and DET measurement results. Therefore, it can be concluded that the proposed method and the ePZT can reliably detect these types of defect on a non-functional DSA.

To correlate the testing performance between ePZT and DET, the statistical analysis of their measurement results was performed. In this example, the number of sample is 1360. It relates the amplitude of 30 mV from ePZT to the 15 micro inch displacement from DET. The distribution of the results is illustrated in Fig. 4.4 and Fig. 4.5 respectively.

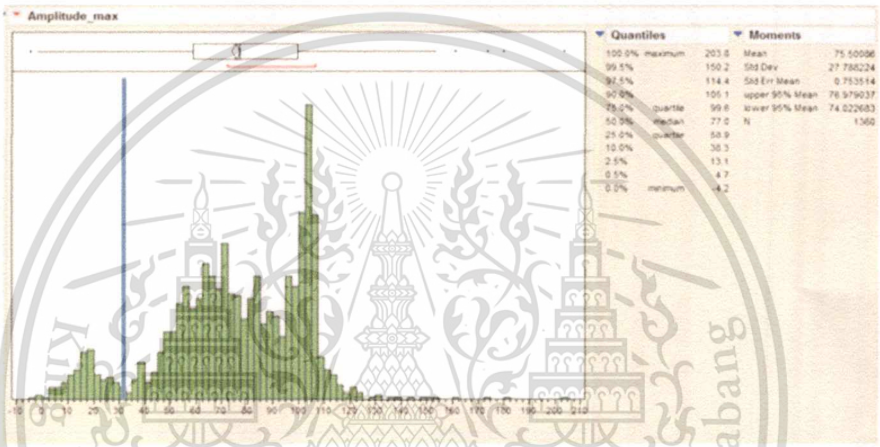

Fig. 4.4 Amplitude distributions from dual stage actuator measurement system

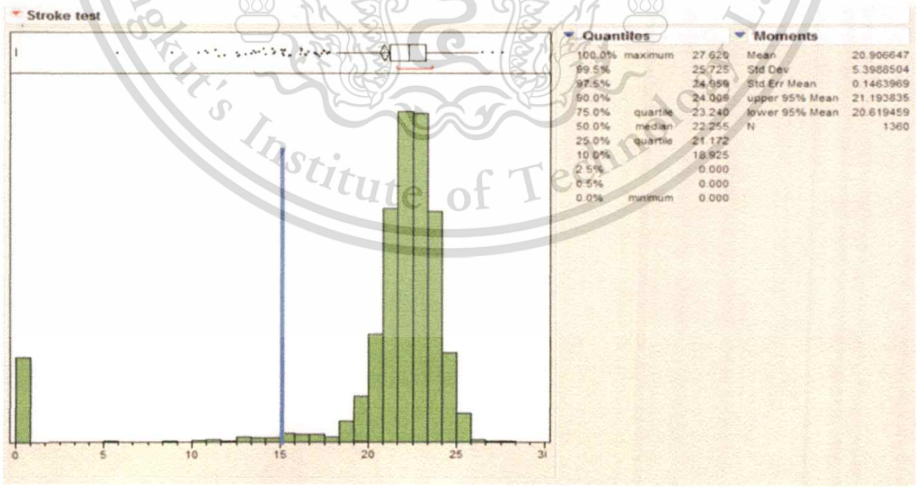

Fig. 4.5 Stroke distributions from dynamic electrical test

Table 4.2 Summary of the test result comparison between DET and dual stage actuator measurement system

KPI (Key parameter indicator)	DET Tester	PZT tester	Gain for PZT tester
Detection rate (improper connectivity)	100%	100%	Comparable
Head failure identify	Yes	Yes	Head failure identify
Test time/unit (min)	5	<1	Eliminate DET
Space required(cm^2)	130	<60	Proper for MFG
Cost/system (K$)	350	<25	Significant low cost system

4.4 Summary

The test method and its measurement system, the ePZT, can detect some types of structural damage to the PZT motors, such as a broken wire bond and some types of fracture motors. Since the DET which performs the stroke test is currently considered as the most accurate and reliable way to measure head performance and identify head failure, it was used as the reference for comparison. The comparison of some key parameter indicators are summarized in Table 4.2. Obviously, in term of identifying DSA-related head failures, the ePZT performance is equivalent to that of DET. Furthermore, when consider in other aspects such as test time per unit, space requirement and cost, using ePZT clearly has more advantages than using DET.

Chapter 5
Conclusion and Future Work

A PZT-actuated suspension failure detector system was designed and tested. The system operation is based on piezoelectric effect. By applying a controllable force to deflect load arm of the HSA suspension, the electrical signal that can provide physical condition of piezoelectric element and its circuit connectivity is generated. Characteristics of the generated signal such as shape and amplitude are used to detect and identify which PZT microactuator of the HSA is degraded and causes a head failure. Test results show that the developed system is not only capable of detecting and identifying the microactuator failure as accurate as the sophisticated DET system but also it is low-cost, requires less space and operates faster than the DET system.

Although the ePZT offers an effective solution for current HSA manufacturing process, there are some improvements that can be done. The automatic spreader pin rotation, for example, can be implemented. Presently, spreader pin is manually rotated to exert force to PZT by the operator. Variation of rotation speed can introduces error, more or less. Thus, a tester with an automatic spreader pin rotation will definitely eliminate this human error and improve productivity such as a higher unit per hour.

Another aspect that needs a careful examination and further research is the type of microactuator which is permissible to use ePTZ's concept. Based on bonding position of the PZT element on HGA, there are three types of microactuator. The type one, PZT element is located near the base plate. This type is used in conventional products. The ePZT was developed based on this structure. In the second type, the type two, PZT element is attached on the load beam between base plate and read/write head. It can be found in new products. Finally, the type three, which will be implemented in the foreseeable future product, its PZT element situates near the read/write head. Accordingly, as the products get more advanced the microactuator moves closer to the read/write head. There is a certain possibility that the concept used in the ePZT design is still applicable to the type two structures. It is challenging, however, to develop techniques that is suitable for

testing the type three. Since it is miniscule and very close to the read/write head, a practical approach should be a non-contact technique.

References

[1] Antonio Arnau Vives, **Piezoelectric Transducers and Applications,** 2nd ED. Springer - Verlag Berlin Heidelberg. Inc 2008.

[2] Hideki Kuwajima, Hirokazu Uchiyama, Yuko Ogawa, Hiroyuki Kita, and Kaoru Matsuoka, **"Manufacturing Process of Piezoelectric Thin-Film Dual-Stage Actuator and Its Reliability for HDD"** IEEE Transactions on Magnetics, Vol. 38, No. 5, Sep. 2002.

[3] Masaru Inoue, Osamu Okawara, and Hideki Fuchino, **"Processing Device for Piezoelectric Actuator and Processing Method for Piezoelectric Actuator",** U.S patent No. 2010/0264934A1, Oct 2010.

[4] Yang Jing, Jianbin Luo, Pengsheng Huang, and Li Qin, **"U-Type Piezoelectric Thin-Film Microactuator for Hard Disk Drives",** IEEE Transactions on Magnetics, Vol. 41, No. 11, Nov. 2005.

[5] Toshiki Hirano and Henry Yang, **"A hard disk drive tracking servo microactuator driven by PZT stroke amplication mechanism",** The 13th International Conference on Solid-state Sensors, Actuators and Microsystems, Seoul, Korea, June 5-9, 2005.

[6] Koganezawa S., Uematsu Y., and Yamada T., **"Dual stage actuator system for magnetic disk drives using a shear mode piezoelectric microactuator",** IEEE Transactions on Magnetics. Vol. 35, No. 2, Mar. 1999.

[7] Li-Yan Zhu, Chao-Hui Yang, Xiaofeng Zhang, and Yen Fu, Cha, **"Method for testing a microactuator in a magnetic tester"** U.S patent No. 7085083B2, Aug. 2006.

[8] Alexei H. Sacks, James H. McGlennen and Albert van der schans, **"Method and apparatus for testing microactuators on a suspension assembly",** U.S patent No. 6510752B1, Jan. 2003.

[9] Wei Guo and Michael R. Hatch, **"Piezoelectric microactuator and sensor failure detection in disk drives",** U.S patent No. 6861854B1, Mar. 2005.

[10] Yuriy Umanskiy, Arnold Shphilberg, Vladimi Vaninskiy, and Eugene Dvoskin, **"Method and apparatus for detecting defects in piezoelectric actuator",** U.S patent No. 6556028B1, Apr. 2003.

[11] Benjamin Acatrinei, **"Piezoelectric interface analyzer",** U.S patent No. 6111335, Aug. 2000.

[12] Yung-Ping Yeh, Marty McCaslin, and C.-P. Roger Ku, **"PZT crack detection in suspension-based dual stage actuator",** IEEE Transactions on Magnetics, Vol. 36, No. 5, Sep. 2000

[13] Jeffrey E. Thomsen, **"Method for detecting piezoelectric element failure in head suspension",** U.S patent No. 6870377B2, Mar. 2005.

[14] Technical TIDBITS, Issue no. 20 – August 2010 **"Cantilever Beams Part 1 - Beam Stiffness"** [Online].
Available : http://materion.com/~/media/Files/PDFs/Alloy/Newsletters

Publication

International Data Storage Technology Conference 2011.

Piezoelectric Microactuator Failure Detector System for Hard Disk Drive

Witthaya Keopuang[1], Kasin Vichienchom[2] and Kitiphol Chitsakul[2]
[1]Western Digital Thailand and College of Data Storage Innovation
King Mongkut's Institute of Technology Ladkrabang, Thailand
[2]Faculty of Engineering
King Mongkut's Institute of Technology Ladkrabang, Thailand

Abstract— **Method and apparatus for detecting failure in a piezoelectric element on a head suspension for a disk drive is described. By clamping one end of the suspension, mechanically displacing and releasing the other end of the suspension produces electrical signal at the output of a piezoelectric element on the suspension. After processed, characteristics of the signal are used to determine defects of its corresponding piezoelectric element and its circuit connectivity. The equipment based on the proposed method, the ePZT, was designed and tested against the Dynamic Electrical Tester (DET). The testing results show that the ePZT provides the same capability as the DET to detect and identify head failure due to its piezoelectric element fracture and broken electrical connection. Moreover, the ePZT possesses several advantages over DET such as low cost, faster operating time, and less space required. Therefore, it is suitable for using in production line.**

Keywords-PZT actuator; dual-state actuator; Microactuator.

I. INTRODUCTION

Hard disk drive (HDD) is the most popular non-volatile, random-access mass data storage. Over the past several years, hard disk drive has been fallen in cost and physical size while dramatically increased in capacity. The biggest lever for higher HDD capacities is to increase both areal density and the number of disk per drive. A single disk can now store about 500 Giga-bytes of data.

Increasing the areal density by reducing data track widths makes it more difficult to locate the read/write head accurately on the data tracks of the disk and keep maintaining. In order to overcome the problem, previous approach was introduction of voice coil motor (VCM), as well as the usage of magnetic disks and head suspension with higher stiffness or rigidity. It is well recognized throughout the industry that these levels of performance cannot be simply achieved by an evolution of the existing voice coil positioning technologies. A feasible solution is to use a dual-stage actuator (DSA). As the first stage control, VCM is still used for track locating. For micro positioning control, the second stage actuator based on piezoelectric structure is employed. This second stage actuator is driven by the signals from the control electronics according to the off-track error. Schematic of a hard disk drive with dual-stage actuator is illustrated in **Fig. 1**. The second stage actuator is mounted on suspension adjacent to read/write head. Its control signals are connected via copper traces on a flexible printed circuit.

Higher number of disks per drive is another method to increase drive capacity. Since data is stored on both sides of the disk therefore it requires two read/write heads per disk. Typically, up to four disks are used thus it can be as much as eight heads and eight micro actuators stack up as shown in **Fig. 2**. To minimize its occupying area, all actuators share the same control signal on the flexible printed circuit. As a result, all piezoelectric circuits are connected in parallel. Since a piezoelectric can be modeled as a capacitor, the equivalent circuit of micro actuators of a head stack assembly (HSA) is a parallel circuit of capacitors as shown in **Fig. 3**.

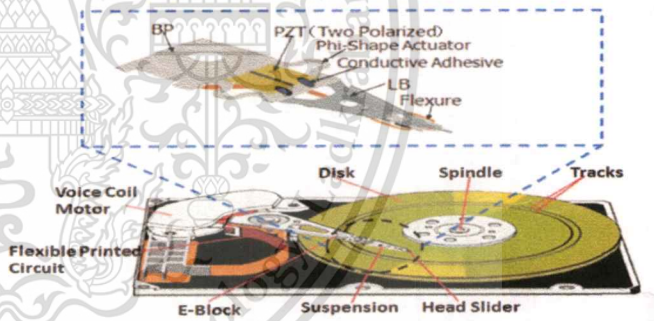

Fig. 1 Schematic of hard disk drive with dual stage actuator. The second stage control using piezoelectric actuator is mounted on suspension adjacent to read/write head

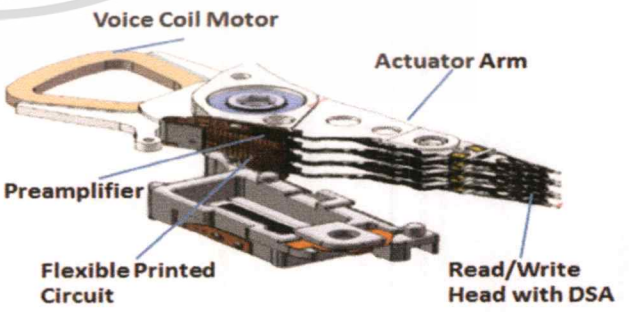

Fig. 2 Head Stack Assembly (HSA)

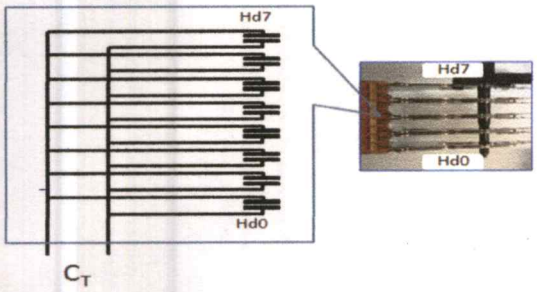

Fig. 3 Micro actuators of a HSA connected in parallel are modeled as a parallel circuit of capacitors.

Physical condition of the piezoelectric structure is directly related to the actuator performance and so the head performance. Conventionally, it can be primarily checked by measuring the value of its capacitance whether it is within its specification. However because of its nature of parallel circuit, only the total capacitance can be measured, thus it is insufficient to identify which piezoelectric is prone to degrade head performance and eventually resulting in head failure.

In this paper the method and apparatus for detecting failure in a piezoelectric element are described. The equipment was designed and tested for production line. The paper is organized as follows. Section II describes the failure and detection of piezoelectric (PZT) actuator. Principle of the operation of the detector system is then explained in Section III. The experimental results are in Section IV. Finally it is summarized in Section V.

II. PZT-ACTUATOR FAILURE AND DETECTION

In HSA manufacturing process, read/write head with its micro actuator is coupled to the drive arm by swaging. The suspension flexure cables which carry the actuator control signal are then electrically connected with the flexible printed circuit assembly (FPCA) by using ultrasonic bonding. Next, the HSA is tested for its electrical connectivity and head performance is measured. This process however also raises two major problems, which contribute to head performance degradation caused by PZT microactuator failure. First, a crack can easily occur inside PZT due to the nature of material when it is subjected to an external loading during the assembly process. This crack degrades the actuator performance and so the head. Second, in some cases due to its fragility of the actuator circuit, it becomes open and fails to operate resulting in the head failure. Consequently, the rework process that requires longer processing time, more space and expensive machine is needed.

To prevent this, PZT failure of HSA need to be detected as early as possible. Detection can be done using either static or dynamic technique. In static technique certain electrical signals are applied to the parallel circuit of PZT then electrical responses are monitor. This technique includes the capacitance measurement, the impedance testing and decay method testing [1-6]. The techniques require no spinning disk thus it is fast, low cost and suitable for a prime production line. However due to its nature of parallel circuits of HSA, the static techniques can detect PZT failure of HSA but can not identify failure at each individual head.

On the other hand, dynamic technique which requires spinning disk performs by applying PZT control signals and then measuring displacement of a corresponding head [7-12]. This method provides a very high accuracy and reliable test result. It can identify which head of the stack fails individually. The process however, is time-consuming and yields low throughput. In addition, the machine cost is very high.

Visual inspection [13] is another viable solution. It has been used in the assembly line. However its lack of repeatability and capability to inspect at the inner heads of HSA make it less attractive.

Mechanical vibration such as ringing method [14] provides an accurate and reliable test result for identifying individual head fail. Nevertheless, it comes with a high risk of degrading suspension. Its long testing time also diminishes the production throughput. Since all available techniques are either costly and time consuming or unable to identify individual head failure, in this research a new testing technique as well as a prototype testing machine has been developed. It not only detects PZT microactuator failure but also identify any defected head of the head stack. This prototype will lead to a low-cost, less processing time and more accurate PZT inspection procedure.

III. PRINCIPLE OF OPERATION

A. Piezoelectric Effect

A piezoelectric substance is one that produces an electric charge when a mechanical stress is applied. This phenomenon is called *direct piezoelectric effect*. Conversely, for the *converse piezoelectric effect*, a mechanical deformation is produced when an electric field is applied.

In the former case, surface density of the generated linked charge is proportional to the pressure exerted, and will disappear with it. This relationship can be formulated in a simple way as follows:

$$P_P = dT \tag{1}$$

Where P_p : piezoelectric polarization
d : piezoelectric strain coefficient
T : stress to which the piezoelectric material is subjected

This can be illustrated conceptually in Fig. 4

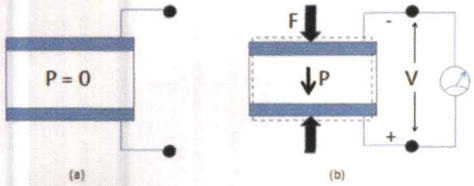

Fig. 4 The piezoelectric effect. (a) A piezoelectric crystal with no applied stress or field. (b) The crystal is strained by an applied force that induces polarization in the crystal and generates surface charges causing voltage difference between electrodes.

The micro actuator is designed and operates based on the converse piezoelectric effect. In its operation, the appropriate control signal is applied to the electrodes of PZT and produces some deformation of the PZT element on the x-y plane as shown in Fig. 5. This deformation causes a micro-scale displacement on the read/write head. During the read/write access, the off-track error is used as a feedback signal to form a closed-loop control system which maintains read/write head at its correct position on the track.

According to the direct piezoelectric effect as described by (1), strain on the PZT element can result in voltage difference between its electrodes. Therefore if a certain amount of external force is applied to the PZT element of the HSA, electrical signal from its electrodes will be detected. Moreover the detected signal of an undamaged PZT and a damaged one should be different. Considering the structure of HSA and its PZT, it is found that a controllable force can be exerted individually on each suspension arm in the z direction. This will create strain only on the PZT element mounted on that arm. Thus electrical signal corresponding to that particular PZT can be observed at the same terminal which is connected to the control signal. The characteristic of this signal can provide information about conditions of PZT element and its circuit connectivity.

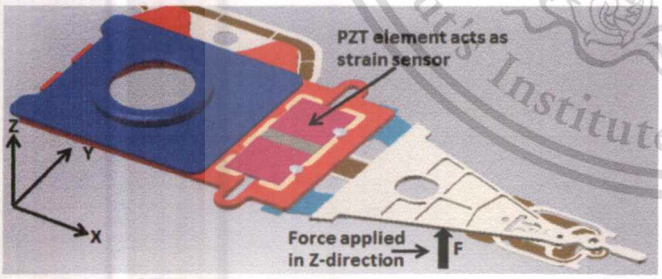

Fig. 5 Piezoelectric element on suspension arm and the reference axis for applying force and its deformation.

B. PZT Microactuator Failure Detector System

The PZT microactuator failure detector system or ePZT has been designed according to the principle explained in previous section. Since it is intended to use as standard equipment in the production line, it must be easy to operate and consume short operating time. The ePZT consists of two main parts. The first part, the front-end fixture, is designed for quick loading of HSA and applying a controllable force to a load beam of the selected read/write head individually. After loading, signals from the flexible printed circuit of HSA are then connected to the second part, the data acquisition and signal processing unit. In this part the analog signal generated by the PZT due to deflection of load beam is amplified and converted to digital signal for further processing. Signal characteristics including shape and its amplitude are recorded and displayed on the data screen. This procedure continues on each head individually until complete all heads. Block diagram of the ePZT is shown in Fig. 6.

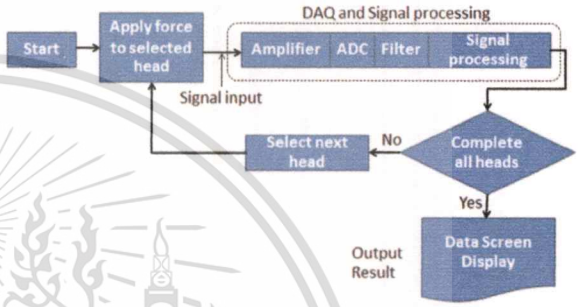

Fig. 6 Diagram of the PZT microactuator failure detector system or ePZT

IV. Experimental Results

To evaluate its performance, ePZT was first tested using HSA with three kinds of condition; HSA with good PZT element, HSA with damaged PZT element (or micro crack) as shown in Fig. 7 and HSA with the open-circuit actuator. The waveforms of signals measured from its actuator circuit are shown in Fig. 8. It can be observed that signals from both good and cracked PZT look similar but different in amplitude. Its positive and negative amplitude are corresponding to the deflecting up and down of the load beam during applying a controllable force. Note that in case of the good PZT element its signal amplitude are noticeable larger than the cracked PZT. For the case of an open circuit, there is no waveform generated.

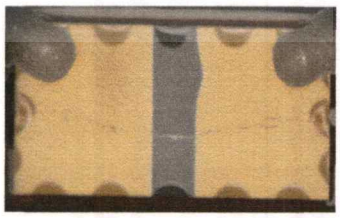

Fig. 7 Microphotograph of the damaged PZT element due to a crack across from left to right.

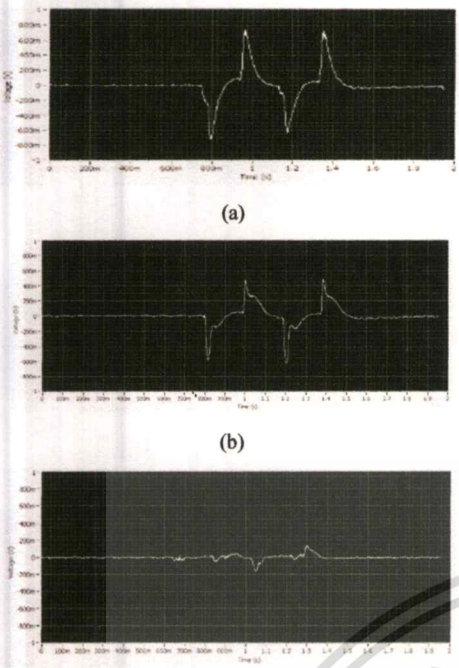

(a)

(b)

(c)

Fig. 8 Waveform of PZT actuator circuits measured by ePZT. (a) a good condition PZT element (b) a PZT element with micro crack and (c) an open-circuit actuator circuit.

Based on these results, one can easily distinguish between these three conditions of the HSA. Next, to qualify ePZT for production line a large number of HSA samples were tested with both ePZT and Dynamic Electrical Testing Machine (DET). Since the DET which performs the stroke test is currently considered as the most accurate and reliable way to measure head performance and identify head failure, it was used as the reference for comparison. The comparison of some key performance indexes is summarized in Table 1. Obviously, in term of identifying head failure due to PZT, the ePZT performance is equivalent to that of DET. Furthermore, when consider in other aspects such as test time per unit, space requirement and cost, using ePZT clearly has more advantages than using DET.

Table 1. Summary of the test result comparison between DET and ePZT

KPI	DET Tester	ePZT	Benefit/Gain for ePZT
Detection rate (improper bonding)	100%	100%	Comparable
Head failure identify	Yes	Yes	Head failure identify
Test time/unit (min)	5	< 1	Eliminate DET
Space required (cm^2)	130	< 60	can use in MFG line
Cost/system(k$)	350	<25	Low cost system

V. Conclusion

A PZT-actuated suspension failure detector system was designed and tested. The system operation is based on piezoelectric effect. By applying a controllable force to deflect load arm of the HSA suspension, the electrical signal that can provide physical condition of piezoelectric element and its circuit connectivity is generated. Characteristics of the generated signal such as shape and amplitude are used to detect and identify which PZT microactuator of the HSA is degraded and causes a head failure. Test results show that the developed system is not only capable of detecting and identifying the microactuator failure as accurate as the sophisticated DET system but also it is low-cost, requires less space and operates faster than the DET system.

Acknowledgement

This work is supported by Western Digital Thailand. The authors would like to thank Raymond Tan, HOD of HSA Product/Test engineer for his support and Dr Yanning Liu, HOD of Mechanical engineering for his valuable suggestion on the topic, and Sanya Thamprasit, Siwaphon Sonkham for experiment supporting.

References

[1] Hideki Kuwajima, Hirokazu Uchiyama, Yuko Ogawa, Hiroyuki Kita, and Kaoru Matsuoka, "Manufacturing process of piezoelectric Thin-film dual-stage actuator and Its reliability for HDD", *IEEE Transactions on Magnetics*, Vol. 38, No. 5, Sep 2002

[2] Eiji Soga, Shingo Tsuda and Kiyoshi Satoh "Apparatus and Method for Fixing and Checking Connection of Piezoelectric Sensor, Actuator and Disk unit", US 6,604,431 B1, Aug 12, 2003.

[3] Benjamin Acatrinei "Piezoelectric interface analyzer" US 6,111,335, Aug. 29,2000.

[4] Yung-Ping Yeh, Marty McCaslin, and C.-P. Roger Ku, "PZT Crack Detection in Suspension-Based Dual Stage Actuator" IEEE Transactions on Magnetics, Vol. 36, No. 5, Sep 2000

[5] Yuriy Umanskiy, Arnold Shpilberg, Vladimir Vanisskiy and Eugene Dvoskin, "Method and Apparatus for Detecting Defects in Piezoelectric Actuators",US 6,556,028 B1, Apr 29, 2003.

[6] D. Mitchel Hanks and Larry S. Mytz, "Method and Apparatus for Testing a Piezoelectric Force Sensor", US. 5,447,051, Sep 5, 1995.

[7] Toshiki Hirano and Henry yang, "A Hard Disk Drive Tracking Servo Microactuator Driven by PZT with Stroke Amplification Mechanism" *IEEE Actuators and Microsystems*, June , 2005.

[8] S. Koganezawa, Y. Uematsu, and T. Yamada, "Shear mode piezoelectric microactuator for magnetic disk drives", *IEEE Transactions on Magnetics*, Vol 34, No. 4, JULY 1998.

[9] Yoshikazu Soeno, Sliinji Ichikawa, Takamitsu Tsuna, Yoshikazu Sato and Isamu Sato "Pizoelectric piggy-back microactuator for hard disk drive", *IEEE Transactions on Magnetics*, Vol. 35, No. 2, Mar 1999

[10] Yang Jing, Jianbin Luo, Pengsheng Huang, and Li Qin, "U-Type Piezoelectric Thin-film Microactuator for Hard disk drive" IEEE Transactions on Magnetics, Vol. 41, No. 11, Nov 2005.

[11] W. Guo, S. Weerasooriya, T.B. Goh, Q.H.Li, C. Bi, K.T. Chang and T.S. Low, "Dual Stage Actuator for High density Rotating Memory devices", *IEEE Transactions on Magnetics*, Vol 34, No. 2, Mar 1998.

[12] S. Koganezawa, Y.Uematsu, and T.Yamada, "Dual-stage actuator system for magnetic disk drives using a shear mode piezoelectric microactuator", *IEEE Transactions on Magnetics*, Vol 35, No. 2, Mar 1999.

[13] H.G. Beom, K.M. Jeong, J.Y. Park, S. Lin and G.H. Kim, "Electrical Failure of Piezoelectric Ceramics with a Conductive Crack under Electric Fields Engineering Fracture Mechanics", Elsevier Ltd 2009.

[14] Jeffrey E. Thomsen "Method for Detecting Piezoelectric Element Failure in Head Suspension" US 6,870,377 B2, Mar 22,2005.